OPEN JOURNAL OF

NANO

ISSN:2147-0081

Volume:7, Issue: 1, Year: 2022

A JOURNAL ABOUT NANOSCIENCE

Volume 7 / Issue 1

Open Journal of Nano

Open Journal of Nano

Editorial Assistants

OPEN JOURNAL OF NANO

Contents
Volume: 7, Issue: 1, Year: 2022

Conformational, Toxic, Physicochemical and Molecular Docking Analysis of the Anticancer Acalabrutinib Molecule 1-9
(Research Article)
Sefa Çelik, **Aliye Demet Demirağ**, Samet Arslan, Aysen E. Özel, Sevim Akyüz

The Effect of Heat Treatments Applied to Continuous Fiber Reinforced Thermoplastic Composites on Mechanical Properties 10-17
(Research Article)
Bahri Barış Vatandaş, Recep Gümrük, Altuğ Uşun, Nuri Yıldız

Investigation of the Use of Marble Powder in Production of High Strength Concretes 18-25
(Research Article)
Tuba Demir, Kürşat Esat Alyamaç

Determination of Metal Content and Biological Activities of Radish Plant Consumed as Turnip by Public in Siirt Region 26-30
(Research Article)
İbrahim Tegin, Bülent Hallaç, Hasan Özden, Mehmet Fidan

Optimization of Cutting Parameters Affecting Cutting Force and Surface Roughness in Machining of AISI P20 Die Steel 31-40
(Research Article)
Mahir Akgün, Barış Özlü

Open Journal of Nano
(2022) 7–1

Conformational, Toxic, Physicochemical and Molecular Docking Analysis of the Anticancer Acalabrutinib Molecule

[1]Sefa CELİK, [2,3]Aliye Demet DEMİRAG, [4]Samet ARSLAN, [1]Aysen E. OZEL, [5]Sevim AKYUZ

[1]Istanbul University, Faculty of Science, Department of Physics, Vezneciler, 34134, Istanbul
[2]Yeditepe University, Vocational School, Internet and Network Technologies Department, 34755, Istanbul
[3]Istanbul University, Institute of Graduate Studies in Sciences, 34452, Istanbul
[4]Yeditepe University, Vocational School, Mechatronic Department, 34755, Istanbul
[5]Istanbul Kultur University, Faculty of Science and Letters, Department of Physics, 34156, Istanbul
Corresponding author, e-mail: demet.demirag@yeditepe.edu.tr

Submission Date: 05.10.2021 Acceptation Date: 12.12.2021

Abstract - Acalabrutinib is an inhibitor of Bruton's tyrosine kinase (BTK) activity and prevents the activation of the B-cell antigen receptor (BCR) signaling pathway. For having these properties acalabrutinib recently was approved for medical use as an anticancer drug. Determining the conformational properties of a bioactive molecule is necessary to reveal its bioactivity. For this reason, the conformational states of the acalabrutinib were examined first. The AM1, a semi-experimental method, was used to examine the stable conformations of the acalabrutinib molecule. Nine lowest energy conformers of the acalabrutinib molecule were determined and their relative energies were calculated. Afterwards, the interactions of the most stable conformer of acalabrutinib with DNA and integrin were examined by docking simulations, and the most active interaction sites and binding affinities were determined.

Keywords: Acalabrutinib, Conformational analysis, Anticancer, Molecular Docking Analysis, Physicochemical Features

1. Introduction

The chemical formula of acalabrutinib (ACP-196) is $C_{26}H_{23}N_7O_2$ and its total weight is 465.5 g / mol. Acalabrutinib is a small molecule and Bruton tyrosine kinase (BTK) inhibitor. BTK is a component of B cell receptor and myeloid cell signaling pathways, and plays multiple roles in the production of autoantibodies. [1]. Therefore, proper control of BTK activity is important for B cell homeostasis. The BTK signal promotes malignant B cell growth and proliferation, as well as the development of malignant cells [2]. BTK inhibitors are of interest for the treatment of cancer. Acalabrutinib binds to BTK in an irreversible manner, blocking the enzyme's cancer-causing activity. In the United States, acalabrutinib was licensed in 2017 as a treatment for refractory mantle cell lymphoma, and in 2019 as a therapy for CLL and small lymphocytic lymphoma. Waldenstrom macroglobulinemia is under evaluation in other malignancies such as pancreatic and non-small cell lung cancer [3].

Although there is currently no definitive treatment for chronic lymphocytic leukemia (CLL), various studies are being conducted to find solutions to long-term response times in chemotherapy treatment and to provide clinical benefit to patients with increasing treatment options. [4-6] Bruton

Thinozine Ibrutinib, the first inhibitor of the kinase (BTK) class, has been used clinically in the treatment of Chronic Lymphocytic Leukemia (CLL), mantle cell lymphoma, and Waldenstrom macroglobulinemia, but since the ibrutinib molecule has various adverse effects on targets other than BTK, researchers are investigating more selective BTK inhibitors [7,8]. Acalabrutinib (ACP-196) is one of the oral inhibitors of Bruton's Tyrosine Kinase (BTK) used in the treatment of B cell malignancies including resistant mantle cell Lymphoma and Chronic Lymphocytic Leukemia.

Chronic Lymphocytic Leukemia (CLL) is the most common type of chronic leukemia that occurs in the elderly people, especially in Europe and America. In this type of leukemia, which progresses rapidly and fatally, the traditional chemotherapy method does not provide a definite improvement [9]. Therefore, researchers, who want to increase the healing process and rate, are working on a number of treatment methods, aimed at the development, proliferation and survival of B cells, which play an important role in the pathogenesis of Chronic Lymphocytic Leukemia (CLL) treatment. We can divide the treatment methods that emerged as a result of the research, into two main groups; the first of these methods is the B-cell receptor (BCR) pathway activated by the stimulation of the micro-environment, the second is the treatment methods targeting the nuclear factor kappa-B (NF-κB) pathway and the cell surface receptor [10]. Ibrutinib, a sub-class of these treatments, is the first orally administered, non-reversible, and selective Bruton Thinozine Kinase inhibitor. It inhibits B cell viability, proliferation and growth and prevents the influence of the tumor microenvironment. The most common side effects during use of ibrutinib are bleeding, rash, and atrial fibrillation [6, 11-14]. After observing these side effects, scientists carried out studies on more selective Bruton Tyrosine Kinase (BTK) inhibitors and focused on Acalabrutinib (ACP-196), one of the more selective second generation Bruton Tyrosine Kinase (BTK) inhibitors.

Acalabrutinib is rationally designed to be more selective and potent than Ibrutinib, with the most important differences showing improved pharmacological properties, including favorable plasma exposure, rapid oral absorption, short half-life, and the absence of irreversible targeting to alternative kinases [9]. Due to these properties, it is named and accepted as a second generation irreversible Bruton Thinozine Kinase (BTK) inhibitor. In theoretical studies on Acalabrutinib, comparation to Ibrutinib was made and this Bruton Thinosine Kinase (BTK) inhibitor showed much less adverse effects on other targets. Acalabrutinib, known as ACP-196, is an FDA-approved therapy and received the title of Orphan Drug to promote treatment of rare diseases. Today, clinical studies are conducted on more than 2500 patients in 40 countries in order to increase the usage areas of Acalabrutinib and to better understand its effects [15]. The reason why a lot of emphasis on side effects are considered are that patients discontinue the treatment due to the adverse effects observed during Ibrutinib treatment. The most common reason for not continuing treatment for chronic lymphocytic leukemia is the emerging side effects [16, 17]. It was predicted that acalabrutinib (ACP-196) could be used twice a day without increasing toxic effects due to its low side effects. Based on this prediction, Phase 1 and Phase 2 studies of Acalabrutinib were conducted at Ohio State University, and as a result of the studies, low rates of side effects such as headache, diarrhea, weight gain, pyrexia, and upper respiratory tract infection were observed in patients. Although the findings of Phase 3 studies on acalabrutinib (ACP-196), a second-generation inhibitor of the Bruton Tyrosine Kinase (BTK) family, are yet unknown, it appears to be promising in the treatment of Chronic Lymphocytic Leukemia (CLL) [18].

In order to reveal the structure-function relationships of the Acalabrutinib molecule due to all these described properties, we performed the conformation analysis in this study and determined the possible conformers and the lowest energy conformation. Molecular docking simulations was performed to determine the interaction of the most stable conformer of Acalabrutinib with DNA and integrin as well as binding affinities and the binding sites. The toxicological and physicochemical properties of Acalabrutinib were also investigated.

2. Materials and Methods

The conformational analysis of the Acalabrutinib molecule was conducted with the help of the Spartan06 software [19] and the AM1 semiempirical quantum mechanical method [20]. The CAVER software [21] was used to predict potential binding sites on the surface of the receptors. Molecular docking investigations were done using AutoDock-Vina software on the identified active sites [22]. A semi-flexible docking protocol, where the ligand (Acalabrutinib) is flexible and target DNA or target protein is rigid, was applied.

The predicted values of the toxicity risks of Acalabrutinib and certain essential physicochemical features are determined using the OSIRIS Property Explorer software [23], which offers the total drug score to estimate the risks.

3. Results and Discussions

3.1. Structure

The conformational analysis of Acalabrutinib revealed nine lowest energy conformers. The relative energies of these nine conformers are tabulated in Table 1. In Figure 1, the molecular modes of these nine most stable conformers of Acalabrutinib are shown.

Table 1. The relative energies of the nine most stable conformation obtained by conformational analysis.

Conformers	Relative energy (kj/mol)
(I)	0
(II)	0.01
(III)	0.01
(IV)	1.03
(V)	1.04
(VI)	2.8
(VII)	4.77
(VIII)	4.79
(IX)	4.93

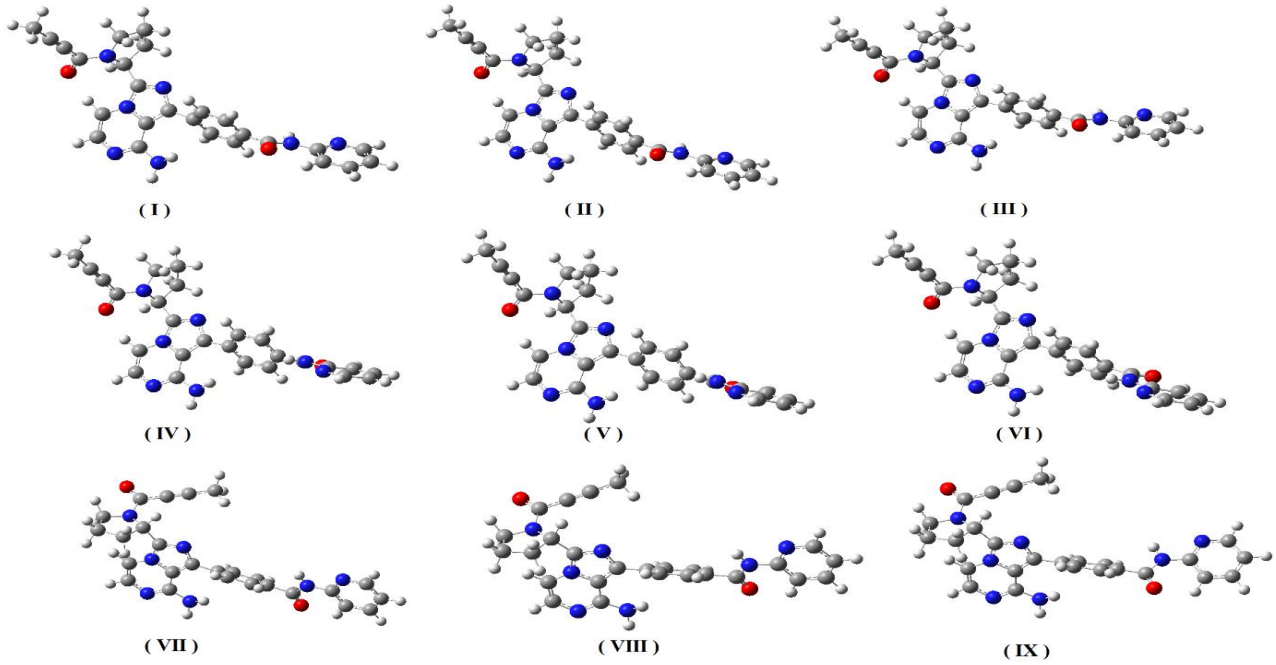

Figure 1. The nine conformers with the lowest energy, obtained by conformational analysis of the Acalabrutinib molecule.

3.2. Molecular Docking

To reveal the interaction mechanism and interaction modes of the anticancer drug Acalabrutinib with DNA and and $\alpha_5\beta_1$ integrin, molecular docking simulations were performed.

The crystal structure of DNA (PDB ID: 1BNA) was acquired with reference to the protein database [24] and the docking studies of the Acalabrutinib molecule was carried out using AutoDockVina [22]. DNA was prepared for the docking study by removing water molecules and adding polar hydrogens, and the DNA charges of Kollman were calculated before the docking study. The Geistenger technique was used to identify the partial charges of the Acalabrutinib molecule, and the active region of DNA was designated as 40Å × 40Å × 40Å grid.

The 3D molecular structure of Acalabrutinib molecule docked in DNA is shown in Figure 2. The most stable conformer of the Acalabrutinib molecule, obtained in gas phase calculations was found to form hydrogen bonds with the nucleic acids DG10 and DG16 (See Figure2) of DNA. The binding affinity (ΔG_{bind}) of Acalabrutinib to DNA is found to be -8.7 kcal/mol, as a result of the calculations. The following are the interactions between the compound Acalabrutinib and nucleic acids:

DG10 and Acalabrutinib molecule: hydrogen bond interactions with lengths of 2.11 and 2.14 Å;

DG16 and Acalabrutinib molecule: hydrogen bond interactions with lengths of 2.06 and 2.47 Å.

In the molecular docking study on cyclo(Ala-His)-DNA by Celik et al., it was found that the peptide interacted with nucleic acids DC9, DG10, DC11, DG16 and DA17 of DNA by hydrogen bonding interactions with 3.1, 2.39, 2.96, 2.53, 2.39 and 2.99 Å lengths, respectively [25]. In another study on molecular docking between 5-chlorouracil (5-FU) and DNA, 5-FU was found to interact with DG10, DC15 and DG16 nucleic acids, through hydrogen bond interactions [26]. Our results are compatible with the previous findings [25-27].

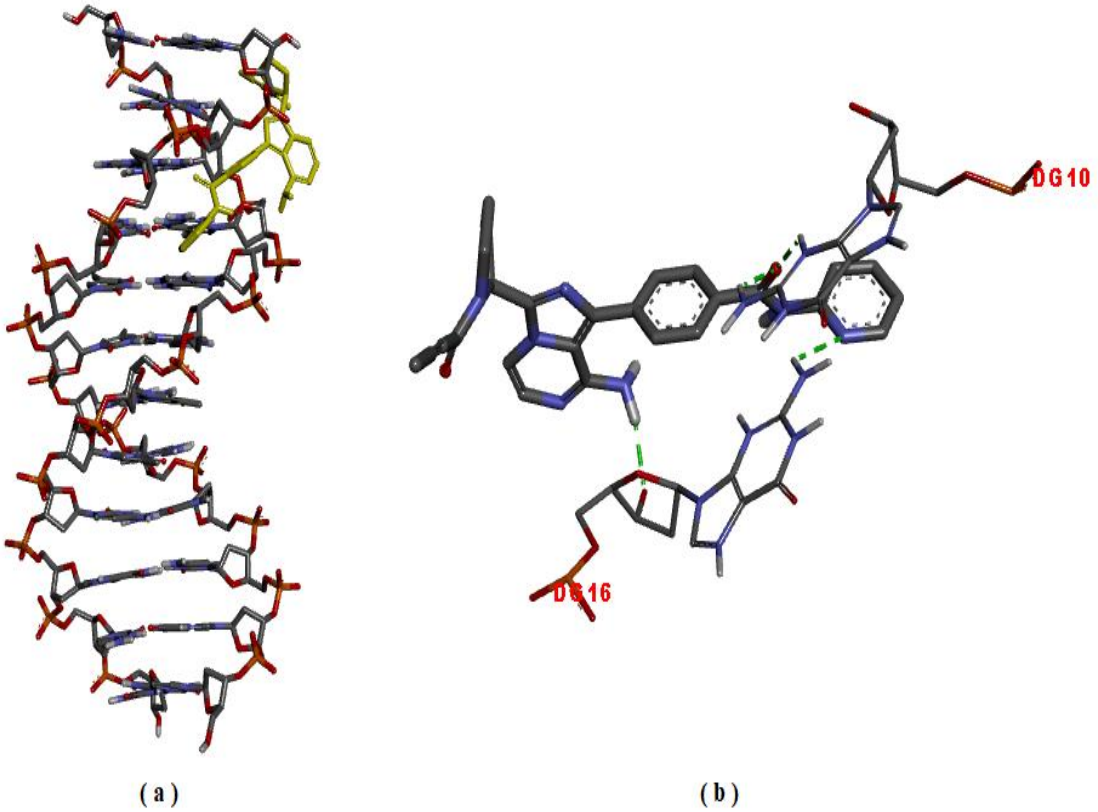

Figure 2. Acalabrutinib docked in DNA (a), The interactions between the ligand and target DNA are labeled using colored dashed lines (b) (ΔG_{bind} = -8.7 kcal/mol).

Molecular docking analyses in the target protein $\alpha_5\beta_1$ integrin were conducted to explore the anti-proliferative impact of Acalabrutinib for anticancer function.

The docking simulations of Acalabrutinib to the $\alpha_5\beta_1$ integrin (PDB ID: 4WK0) were done for the most active site after the $\alpha_5\beta_1$ integrin (PDB ID: 4WK0) was prepared for molecular docking [28]. The most efficient binding was discovered in the active site of the $\alpha_5\beta_1$ integrin, with a binding affinity of -10.7 kcal/mol. Figure 3 depicts the 3D view of Acalabrutinib docked in $\alpha_5\beta_1$ integrin and the amino acid residues involved in the interactions with the ligands are shown.

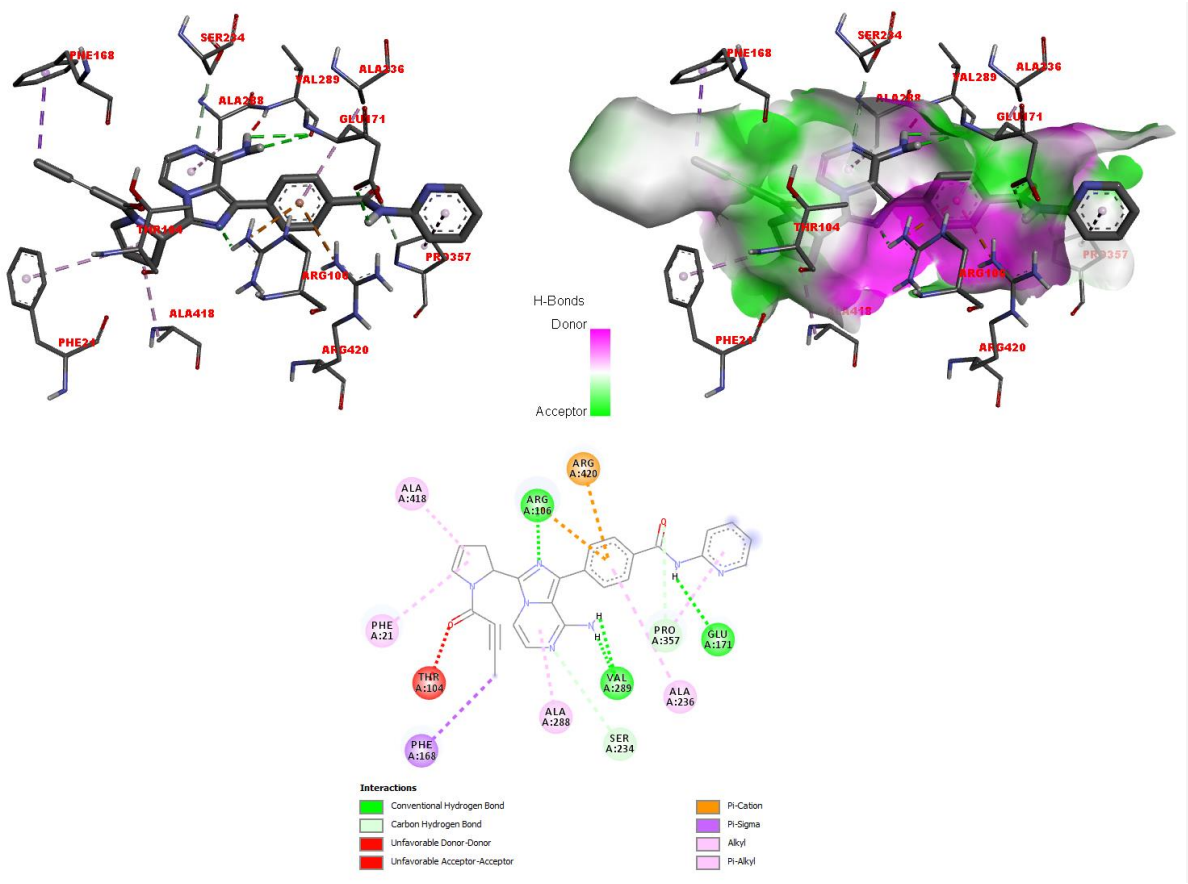

Figure 3. The 3D docked view of the most stable conformer of Acalabrutinib in active site of $\alpha_5\beta_1$ integrin (-10.7 kcal/mol). The interacted amino acid residues with the ligand are shown.

The interactions between Acalabrutinib and residues marked in Figure 3 are given below:

5.2Å long Pi-Alkyl interaction with **Phe21;** 2.87 Å long unfavorable acceptor-acceptor interaction with Thr104; 2.09 Å long hydrogen bond and 4.07 Å long Pi-cation interaction with **Arg106;** 3.83 Å long Pi-Sigma interaction with **Phe168**; 2.45 Å long hydrogen bond with **Glu171**; 3.62 Å long carbon hydrogen bond with **Ser234**; 5.32 Å long Pi-Alkyl interaction with Ala236; 4.51 Å long Pi-Alkyl interaction with Ala288; 1.46 Å long unfavorable donor-donor interaction with Val289 and 2.97, 2.99 Å long hydrogen bonds; 3.44 Å long carbon hydrogen bond and 4.81 Å long Pi-Alkyl interaction with Pro357; Interaction of Ala418 with 4.56 Å long Alkyl; Pi-cation interaction with Arg420 at a length of 4.1 Å.

In the previous study on the interaction of cationic pentapeptide Glu-Gln-Arg-Pro-Arg with $\alpha_5\beta_1$ integrin it was reported that pentapeptide interacted with the Phe21, Ser22, Val23, Arg106, Phe168, Glu171, Ser234, Val235, Lys269, Tyr287, Leu355, Ser417, Arg420 amino acids of integrin by salt bridge, attractive charge, hydrogen bond, carbon hydrogen bond, unfavorable positive-positive,

unfavorable donor-donor interactions [29]. The common amino acids indicate that Acalabrutinib molecule docked into the same active site of integrin where cationic pentapeptide docked.

The Molecular Mechanics Poisson-Boltzmann Surface Area (MM/PBSA) and the molecular mechanics generalized Born surface area (MM/GBSA) approaches are generally used to estimate the binding free energy of small ligands to biological macromolecules [30-35]. Due to the importance of both MM/PBSA and MM/GBSA approaches, Wang [30] developed a program which combined both methods as MM/PB(GB)SA approach. In this study the binding free energies of Acalabrutinib with DNA and $\alpha_5\beta_1$ integrin, were calculated using the program developed by Wang [30], based on MM/PB(GB)SA approach.

The predicted binding free energy of Acalabrutinib with DNA and with $\alpha_5\beta_1$ integrin were obtained as -12.73 and -11.46 kcal/mol, respectively by using the MM/PB(GB)SA approaches with the GAFF2 and ff14SB force field combination and the GB6 procedure [30].

3.3. Analysis of toxicological and physicochemical properties of Acalabrutinib

Acalabrutinib's drug-likeness properties were computed using OSIRIS (2010), and the findings are given in Table 2. The toxicity risk predictor indicates that there are no hazards of mutagenicity, tumorigenicity, irritant, or reproductive problems with this compound.

CLogP is a critical parameter in drug development and environmental toxicity studies, and it must not exceed 5.0 [23]. The absorption and distribution characteristics of a drug in aqueous solution are influenced by its solubility (logS) qualities. The logS-based OSIRIS method is used to evaluate a compound's solubility. More than -4 [23] is the recommended value. The molecular features of the promoted drugs are used to characterize drug-likeness. The total of the molecular score values of the fragments present determines the drug-likeness.

Table 2. Osiris's estimation of title compounds toxicity hazards and physicochemical properties.

Compound	Toxicity risks			
	Mutagenic	Tumorigenic	Irritant	Reproductive Effect
Acalabrutinib	no indication	no indication	no indication	no indication
	Physicochemical properties			
	cLogP	Solubility	Druglikeness	Drug-score
	2.68	-7.19	-2.38	0.23

4. Conclusions

In this work, conformational analysis of Acalabrutinib, an inhibitor of Bruton's tyrosine kinase (BTK) activity and an approved for medical use as an anticancer drug, was performed by a semi-experimental AM1 conformational study, to determine its most stable conformer. Since the protein-ligand interactions are significant in drug design, docking simulations were used to evaluate the biological activity of the most stable conformer of Acalabrutinib. As a result of molecular docking estimates, the binding affinities of Acalabrutinib to DNA and $\alpha_5\beta_1$ integrin were obtained as -8.7 and -10.7 kcal/mol, respectively. The presence of inhibitory activity of the Acalabrutinib ligand indicates that this ligand has good anti-tumor properties. In addition, the physicochemical properties of Acalabrutinib also show that the molecule has good pharmacokinetic profiles.

Peer-review: Externally peer - reviewed.

Financial Disclosure: The authors declared that this study has received no financial support (If there is financial support, please specify the grant organization and support number).

References

1. Satterthwaite A.B. Bruton's Tyrosine Kinase, a Component of B Cell Signaling Pathways, Has Multiple Roles in the Pathogenesis of Lupus, Frontiers in Immunology, 8 (2018) 1-10. Article No 1986. DOI: 10.3389/fimmu.2017.01986
2. "Acalabrutinib Monograph for Professionals". Drugs.com. Retrieved 16 March 2019.
3. Barf, T., Covey, T., Izumi, R., van de Kar, B., Gulrajani, M., van Lith, B., ... & Kaptein, A. (2017). Acalabrutinib (ACP-196): a covalent Bruton tyrosine kinase inhibitor with a differentiated selectivity and in vivo potency profile. Journal of Pharmacology and Experimental Therapeutics, 363(2), 240-252.
4. Goede V, Fischer K, Busch R, Engelke A, Eichhorst B, Wendtner CM, et al. Obinutuzumab plus chlorambucil in patients with CLL and coexisting conditions. N Engl J Med. 2014;370(12):1101–10.
5. Cang S, Iragavarapu C, Savooji J, Song Y, Liu D. ABT-199 (venetoclax) and BCL-2 inhibitors in clinical development. J Hematol Oncol. 2015;8(1):129.
6. Novero A, Ravella PM, Chen Y, Dous G, Liu D. Ibrutinib for B cell malignancies. Experimental Hematology & Oncology. 2014;3(1):1–7.
7. Covey T, Barf T, Gulrajani M, Krantz F, van Lith B, Bibikova E, et al. Abstract 2596: ACP-196: a novel covalent Bruton's tyrosine kinase (Btk) inhibitor with improved selectivity and in vivo target coverage in chronic lymphocytic leukemia (CLL) patients. Cancer Res. 2015;75(15 Supplement):2596.
8. Walter HS, Rule SA, Dyer MJS, Karlin L, Jones C, Cazin B, et al. A phase 1 clinical trial of the selective BTK inhibitor ONO/GS-4059 in relapsed and refractory mature B-cell malignancies. Blood. 2016;127(4):411–9.
9. The New England Journal of Medicine 374;4 nejm.org January 28, 2016
10. Ferit Avcu, Kll Tedavisinde Gelecek: Hedefe Yönelik Yeni Moleküller XXXIX. Ulusal Hematoloji Kongresi
11. Treon SP, Tripsas CK, Meid K, Warren D, Varma G, Green R, et al. Ibrutinib in previously treated Waldenstrom's macroglobulinemia. N Engl J Med. 2015; 372(15):1430–40.
12. Byrd JC, Furman RR, Coutre SE, Flinn IW, Burger JA, Blum KA, et al. Targeting BTK with ibrutinib in relapsed chronic lymphocytic leukemia. N Engl J Med. 2013;369(1):32–42.
13. Brown JR, Barrientos JC, Barr PM, Flinn IW, Burger JA, Tran A, et al. The Bruton tyrosine kinase inhibitor ibrutinib with chemoimmunotherapy in patients with chronic lymphocytic leukemia. Blood. 2015;125(19):2915–22.
14. Burger JA, Tedeschi A, Barr PM, Robak T, Owen C, Ghia P, et al. Ibrutinib as initial therapy for patients with chronic lymphocytic leukemia. N Engl J Med. 2015;373(25):2425–37.
15. https://pubchem.ncbi.nlm.nih.gov/compound/71226662
16. Maddocks KJ, Ruppert AS, Lozanski G, et al. Etiology of ibrutinib therapy dis- continuation and outcomes in patients with chronic lymphocytic leukemia. JAMA Oncol 2015;1:80-7.
17. Jain P, Keating M, Wierda W, et al. Outcomes of patients with chronic lym- phocytic leukemia after discontinuing ibrutinib. Blood 2015;125:2062-7.

18. ClinicalTrials.gov number, NCT02477696

19. Shao, Y., Molnar, L. F., Jung, Y., Kussmann, J., Ochsenfeld, C., Brown, S. T., ... & DiStasio Jr, R. A. (2006). Advances in methods and algorithms in a modern quantum chemistry program package. Physical Chemistry Chemical Physics,8(27), 3172-3191.

20. Devar, M.J.S.;Zoebisch, E.G.; Healy, E.F.; Stewart, J.J.P. AM1: A new General purposequantum mechanical molecular model.J. Am. Chem. Soc.1985, 107, 3902-3909.

21. Jurcik, A.; Bednar, D.; Byska, J.; Marques, S.M.; Furmanova, K.; Daniel, L.;... Pavelka, A. CAVER Analyst 2.0: analysis and visualization of channels and tunnels in protein structures and molecular dynamics trajectories. *Bioinformatics* **2018**, 34, 3586-3588.

22. Trott, O.; Olson, A.J. AutoDock Vina: Improving the speed and accuracy of docking with a new scoring function, efficient optimization, and multithreading.J. Comput. Chem. 2010,31, 455-461.

23. OSIRIS. (2010).OSIRIS Property Explorer. Actelion Pharmaceuticals Ltd. http://www. https://www.organic-chemistry.org/prog/peo/

24. Drew, H. R., Wing, R. M., Takano, T., Broka, C., Tanaka, S., Itakura, K., &Dickerson, R. E. (1981). Structure of a B-DNA dodecamer:Conformation and dynamics.Proceedings of the National Academy ofSciences,78(4), 2179–2183.

25. Celik, S., Yilmaz, G., Ozel, A. E., & Akyuz, S. (2020). Structural and spectral analysis of anticancer active cyclo (Ala–His) dipeptide. *Journal of Biomolecular Structure and Dynamics*, 1-13.

26. Akalin, E., Celik, S., & Akyuz, S. (2020). Molecular Modeling, Dimer Calculations, Vibrational Spectra, and Molecular Docking Studies of 5-Chlorouracil. Journal of Applied Spectroscopy, 86(6), 975-985.

27. Arif, R., Rana, M., Yasmeen, S., Khan, M. S., Abid, M., & Khan, M. S. (2020). Facile synthesis of chalcone derivatives as antibacterial agents: Synthesis, DNA binding, molecular docking, DFT and antioxidant studies. Journal of Molecular Structure, 1208, 127905.

28. W. Xia, T.A. Springer, Metal ion and ligand binding of Integrin α5β1, PNAS 111 (2014) 17863-17868, http://doi.org/10.1073/pnas.1420645111.

29. Gasymov, O. K., Celik, S., Agaeva, G., Akyuz, S., Kecel-Gunduz, S., Qocayev, N. M., ... & Aliyev, J. A. (2021). Evaluation of anti-cancer and anti-covid-19 properties of cationic pentapeptide Glu-Gln-Arg-Pro-Arg, from rice bran protein and its d-isomer analogs through molecular docking simulations. Journal of Molecular Graphics and Modelling, 108, 107999.

30. Wang, Z., Wang, X., Li, Y., Lei, T., Wang, E., Li, D., ... & Hou, T. (2019). farPPI: a webserver for accurate prediction of protein-ligand binding structures for small-molecule PPI inhibitors by MM/PB (GB) SA methods. Bioinformatics, 35(10), 1777-1779.

31. Hao, G. F., Jiang, W., Ye, Y. N., Wu, F. X., Zhu, X. L., Guo, F. B., & Yang, G. F. (2016). ACFIS: a web server for fragment-based drug discovery. Nucleic acids research, 44(W1), W550-W556.

32. Hao, G. F., Wang, F., Li, H., Zhu, X. L., Yang, W. C., Huang, L. S., ... & Yang, G. F. (2012). Computational discovery of picomolar Q o site inhibitors of cytochrome bc 1 complex. Journal of the American Chemical Society, 134(27), 11168-11176.

33. Yang, J. F., Wang, F., Jiang, W., Zhou, G. Y., Li, C. Z., Zhu, X. L., ... & Yang, G. F. (2018). PADFrag: a database built for the exploration of bioactive fragment space for drug discovery. Journal of chemical information and modeling, 58(9), 1725-1730.

34. Cheron, N., Jasty, N., & Shakhnovich, E. I. (2016). OpenGrowth: an automated and rational algorithm for finding new protein ligands. Journal of medicinal chemistry, 59(9), 4171-4188.

35. Wang, E., Sun, H., Wang, J., Wang, Z., Liu, H., Zhang, J. Z., & Hou, T. (2019). End-point binding free energy calculation with MM/PBSA and MM/GBSA: strategies and applications in drug design. Chemical reviews, 119(16), 9478-9508.

The Effect of Heat Treatments Applied to Continuous Fiber Reinforced Thermoplastic Composites on Mechanical Properties

[1] Bahri Barış VATANDAŞ, [2] Recep GÜMRÜK, [3] Altuğ UŞUN, [4] Nuri YILDIZ

[1] Karadeniz Technical University, Mechanical Engineering Depart., Trabzon, Turkey.
Corresponding author, e-mail: brsvtnds@hotmail.com
[2] Karadeniz Technical University, Mechanical Engineering Depart., Trabzon, Turkey.
e-mail: rgumruk@ktu.edu.tr
[3] Karadeniz Technical University, Mechanical Engineering Depart., Trabzon, Turkey.
e-mail: altug@ktu.edu.tr
[4] Karadeniz Technical University, Mechanical Engineering Depart., Trabzon, Turkey.
e-mail: sinognuri@gmail.com

Submission Date: 08.12.2021 Acceptation Date: 17.01.2022

Abstract - This study investigated the effects of different heat treatments on continuous fiber-reinforced thermoplastic (CFRTP) 's. CFRTP composite is produced using fused deposition modeling (FDM), which is one of the additive manufacturing methods. Polylactic acid (PLA) was used as a matrix, and carbon fibers (3K) were utilized as reinforcement material. First, CFRTP filament was produced on a specially designed melt impregnation line. Afterward, test samples were manufactured via a conventional 3D printer. Then, heat treatments (re-melting in salt, microwave oven, oven) were applied to the produced samples, and the effects of these processes on mechanical properties were investigated. Three-point bending tests were used to investigate the mechanical properties of the test samples. As a result of the heat treatments applied to the CFRTP specimens, flexural stresses between 200 and 220 MPa was achieved. The highest bending stress was obtained by re-melting in salt. As a result of the heat treatments, the stress values are similar, but the re-melting in salt application exhibited a more rigid behavior.

Keywords: Continuous Fiber Reinforced Thermoplastic; Heat Treatment; 3D Printing; Fused Deposition Modeling

1. Introduction

3D printers, also known as additive manufacturing (AM) methods, are a technology that enables computer-generated models to be converted into physical parts [1]. AM technology produces lightweight parts, uses less material waste [2], and it is possible to obtain complex geometries. For this reason, it is preferred in the production of parts in many industries such as aviation, medical and automotive [3]. Although more innovations and improvements are made in the AM method, some disadvantages are encountered in this method [4]. For example, the low mechanical, physical, and thermal properties of the printed parts are among the main disadvantages of the AM method. In order to improve the mechanical properties of the parts, many methods have been used, such as selecting the best printing parameters [5–7], adding reinforcements [8-9], applying heat treatment [10–12], etc., in the literature.

It has been observed that the mechanical properties of the parts produced by optimizing the printing parameters are affected mainly by the printing temperatures, printing speed, layer thickness, scanning angle, fill rate, etc.

[1] Corresponding author: Tel: 0 537 465 76 15
E-mail: brsvtnds@hotmail.com

For example, Gunay et al. [13] prepared PLA+ samples produced by a 3D printer according to various printing parameters and examined the effects of these parameters on tensile strength. As a result, the most important parameters were fill rate, raster angle, and printing speed, respectively. Similarly, Ning et al. [14] The effects of process parameters (raster angle, infill speed, nozzle temperature, and layer thickness) on mechanical properties were investigated using chopped carbon fiber reinforced ABS composite filament. As a result, the highest mechanical properties were obtained with 0, 90 printing angle, 25 mm/s infill speed, 220°C nozzle temperature, 0.25 mm layer thickness.

Although many studies have been done on optimizing printing parameters [7], the improvements obtained with this method have been limited. Different studies have been carried out to improve the mechanical properties, apart from optimizing the printing parameters. For example, Jo et al. [15] subjected PLA samples produced with a 3D printer to heated under high pressure in a hot stamping die. He investigated the changes in the mechanical properties of the samples with the effects of heating and pressure and obtained higher mechanical results than the untreated sample. The reason for this was interpreted as the decrease in the voids in the internal structure of the piece. Also, Nakagawa et al. [16] laid the carbon fibers on the pure polymer parts while printing and produced a sandwich structure with the help of a hot pin. Then, these samples were subjected to heat treatment in a microwave oven to increase the adhesion between the fiber matrix and improve the mechanical properties. As a result, it was observed that the mechanical properties were affected insignificantly because the bond between the fiber and the matrix is weak due to the preparation method of the samples, and the application of microwave heat treatment removed a small number of voids in the internal structure.

Another method to improve mechanical properties is the addition of various reinforcement elements to the polymer material. Continuous fiber-reinforced thermoplastic composite (CFRTP) has been shown to exhibit extraordinary mechanical properties compared to non-reinforced polymer and/or short fiber-reinforced parts. For example, Caminero et al. [17] produced continuous glass, carbon, and Kevlar® fiber reinforced nylon composites using fused deposition method (FDM) technology. The interlayer adhesion performance of these samples was investigated. As a result, it was seen that the mechanical properties of the composite samples were higher than the pure samples. In a similar study, Matsuzaki et al. [18] produced composite samples using the PLA thermoplastic filament and carbon fiber/jute fiber reinforcement element by impregnating a hot nozzle before printing. Pure and composite samples were subjected to mechanical tests to measure tensile strength. The results obtained showed that the highest tensile strength was the PLA composite sample with carbon fiber reinforcement. Although superior mechanical properties are obtained in the parts produced by the additive CFRTP method, gaps in the internal structure, weak interlayer adhesion, etc., limit the mechanical properties of the parts produced by this method [19].

In this study, heat treatments were applied to CFRTP samples to increase the mechanical properties. For this purpose, a melt impregnation line method was utilized to produce CFRTP filaments. Then, an FDM-type 3D printer was used to prepare the samples using the produced filaments. Next, oven, microwave oven, and salt-remelting methods were applied to the printed parts. First, the oven and microwave methods were used to bring the printed parts to the glass transition temperature to increase interlayer bonding. Then, the CFRTP sample was placed in fine salt and heat-treated in the oven at melting temperatures in the salt re-melting method. The main advantage of this heat treatment is that it can also be applied to complex geometries. After the heat treatment methods, mechanical properties were investigated using three-point bending tests.

2. Materials and Methods

2.1 Materials

Continuous carbon fiber (3K, DowAksa, Turkey) was used in this study. Carbon fibers have a tensile strength of 4900 MPa and a modulus of elasticity of 245 GPa, and a density of 1.8 g/cm3. Therefore, the approximate diameter of each strand is 7 µm. In addition, 1.75 mm PLA (Polylactic acid) filament (Porima, Turkey) with a tensile strength of 54.3 MPa and a modulus of elasticity of 2300 MPa was used as a matrix material.

2.2 CFRTP Filament Manufacturing

Initially, a production line based on the melt impregnation method was used to produce the CFRTP filaments. The schematic image of the production line used in our study is shown in Figure 1 [20]. This line consists of the fiber spreading zone, the polymer blend, and finally, the mold. The fiber-spreading zone is formed by positioning multiple rollers to spread the fibers laterally to ensure uniform impregnation of the fibers. The positions of the rollers are designed to be adjustable to change the tensile force on the fiber. In this way, the spread of the fibers is made possible by the tensile force created. If the applied force is excessive, it may break the fiber strands, and if it is not enough, sufficient spreading will not occur. The second zone of the production line aims to impregnate the molten polymer with the dispersed fiber. For this purpose, the guiding rollers in this region were heated to 210°C with cartridges. The PLA filament is mixed with the fiber strip by a polymer-fiber mixture roller. The filaments are pushed into the melting zone by means of the extruder. The polymer mixture roller has a channel passing through the middle of the cylinder to guide the polymer. A total of seven radial (for a homogeneous mixture) holes, each with 0.6 mm in diameter, were drilled on the surfaces of the cylinder where it contacts with the fiber. The molten polymer flows through these holes and meets the fiber, and the mixture is obtained. Finally, a circular heated nozzle was used to transform the produced composite filament into a circular form to be used in the 3D printer. The fiber ratios of the produced filaments were calculated with the same principle as in our previous study [20]. As a result of the calculations, the fiber ratios were kept at 23%.

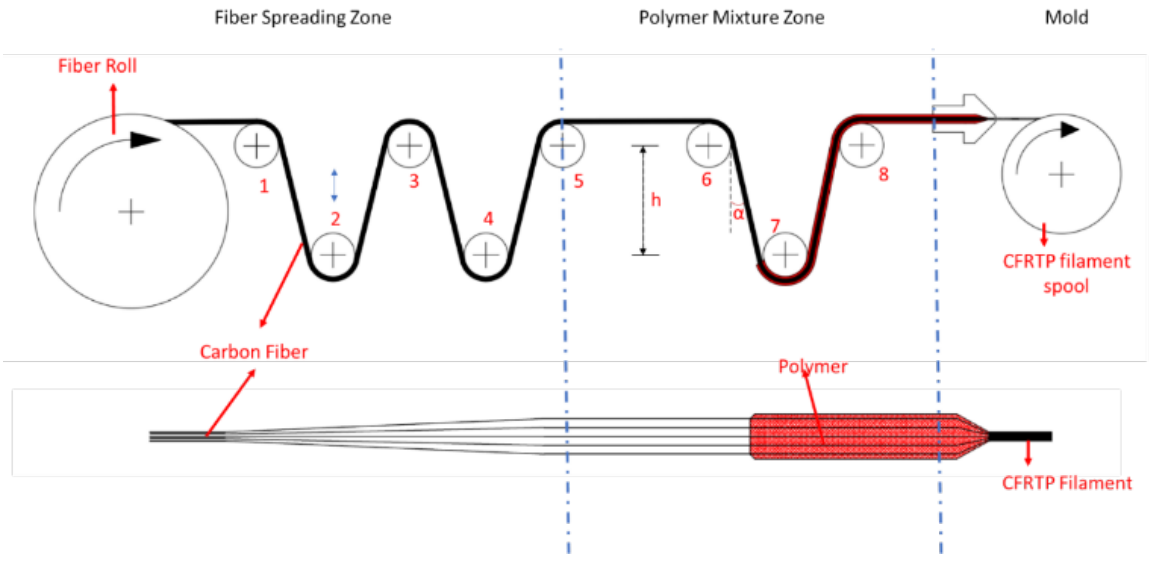

Figure 1. The schematic image of the production line [20]

2.3 Additive Production of CFRP Sample

The 3D printer shown in Figure 2a was used to produce the test samples. In addition, a special g-code was issued for the CFRTP thermoplastic filament to be used in the manufacturing of mechanical test samples. All the samples were produced with continuous pathing, and no cutting was required. However, standard nozzles used in 3D printers have been found to cause fiber damage during printing. For this reason, the nozzle tip used in the study was rounded, and the hole diameter was drilled as 2 mm (larger than the filament diameter). In addition, 220°C nozzle temperature, 10 mm/s printing speed, and 0.25 mm layer thickness were selected as printing parameters. The images of the produced samples are shown in Figure 2b.

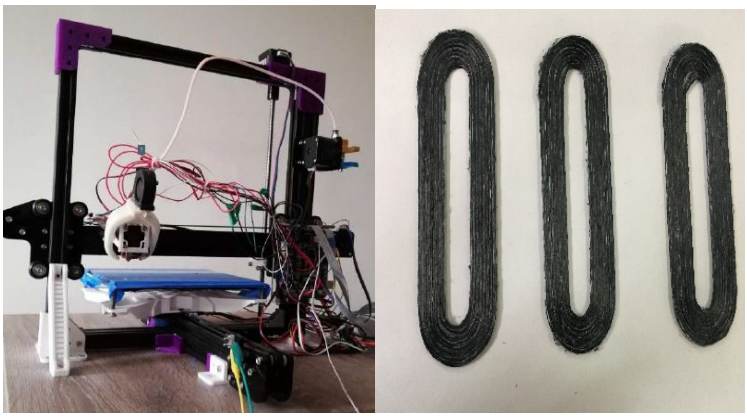

(a) (b)

Figure 2. Additive manufacturing of CFRTP samples; a) Custom 3D printer and b) Bending Test Specimens

2.4 Heat Treatments

The heat treatment methods and parameters used in this study can be summarized as; 100°C and 75 min in oven heat treatment, 210°C and 125 min in salt re-melting, and 300 W and 10 min microwave heat treatment. Oven heat treatment was carried out in a furnace. The three-point bending samples produced from the 3D printer are placed directly into the furnace and kept at 100 °C for 75 min. Next, CFRTP samples were placed in the mold with fine salt in the salt re-melting heat treatment. Samples embedded in salt with 210°C for 75 min. The samples were then removed from the oven and cleaned. Finally, samples were merged in water in the microwave oven heat treatment to prevent arcing because of the conductive carbon fibers. In this method, parts were kept in the microwave with 300 W for 10 min. The preparation of the samples before each heat treatment method is shown in Figure 3.

(a) (b) (c)

Figure 3. Preparation of CFRTP samples for heat treatment; a) Re-melting in the salt sample, b) Microwave sample, and c) Oven sample.

2.5 Tree-point bending tests

In this study, the bending properties of the CFRTP samples were investigated. The MTS Criterion Model 45 tester (figure 4) was used for the bending test. The samples were produced in accordance with the parameters of the "ISO 14125 - Determination of Flexural Properties of Fiber Reinforced Plastic Composites" standard. For the three-point bending tests, samples were prepared with dimensions of 100x15x2 mm. The crosshead velocity in the device was used as 5 mm/min. The tests were repeated four times to prove reproducibility.

Figure 4. Application of three-point bending tests on CFRTP samples

3. Results and Discussions

Bending stress-strain curves obtained from three-point bending tests of CFRTP composites are shown in Figure 5. As seen in the figure, re-melting in salt showed the highest flexural modulus of elasticity and flexural strength compared to the untreated and pure samples. In the salt re-melting method, interfacial gaps formed during printing are reduced when the melting point of the matrix is reached. The effect of microwave heat treatment has shown negative results, and obtained stress values were lower when compared with non-heat treated CFRTP samples. This is possibly caused by the addition of water which caused shorter cooling times and prevented heating of the parts. All results for the three-point bending test are summarized in Table 1. Oven, Salt re-melting, Microwave test specimens provided flexural stress of 217, 218, 203 MPa and a modulus of elasticity of 12, 16, 15 GPa, respectively. Untreated and neat PLA test specimens provided bending stress of 205,89, 61,90 and a modulus of elasticity of 14,56 and 2,07 GPa, respectively.

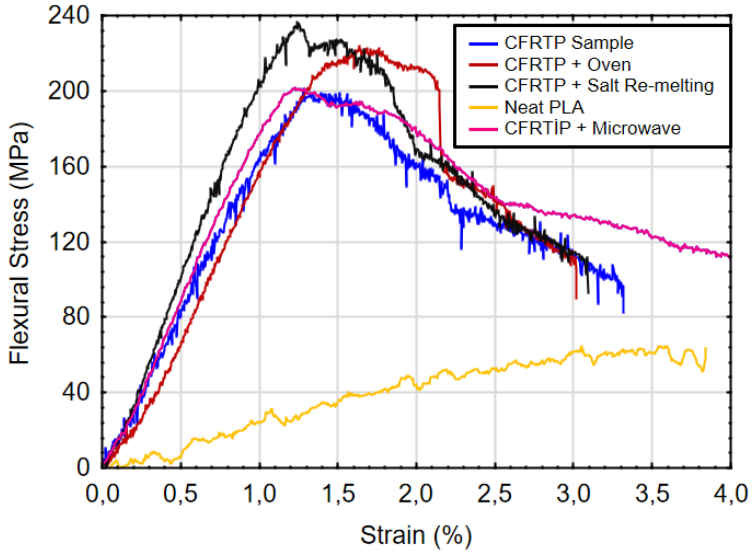

Figure 5. Three-point bending stress-strain curves of CFRTP samples

Table 1. Summary of three-point bending test results

Production Method	Flexural Strength (MPa)	Increase in Flexural Strength (%)	Flexural Modulus of elasticity (GPa)	Increase in Flexural Modulus of Elasticity (%)
Neat PLA	61,90 (4,91)	-	2,076 (1,38)	-
CFRTP Sample	205,89 (7,23)	233	14,56 (1,48)	601,3
CFRTP + Oven	217,04 (11,74)	251	12,16 (3,71)	485,7
CFRTP + Microwave	202,58 (10,50)	227	15,78 (2,20)	660,1
CFRTP + Re-melting Salt	217,72 (34,34)	252	16,15(4,41)	677,9

** Standard deviation is given in brackets.*

4. Conclusions

In this study, CFRTP filament was produced using a melt impregnation line. Three-point bending test samples were printed on an FDM-based additive manufacturing platform from these filaments. Test samples were subjected to three different heat treatments. Then, its mechanical properties were examined by a three-point bending test. The re-melt process yielded a peak bending strength of 217.72 MPa. An increase of 251.79% compared to the neat PLA test sample was achieved. On the other hand, microwave oven heat-treated samples achieved the lowest flexural strength of 202.58 MPa. In future work, mechanical properties can be improved by applying different heat treatments (hot press, etc.) or thoroughly investigating heat treatment parameters.

Peer-review: Externally peer - reviewed.

Author contributions: Writing - Review & Editing, Methodology – B.B.V., A.U.; Conceptualization – A.U.; Visualization B.B.V.; Investigation B.B.V, A.U., N.Y.; Supervision- R.G.; Literature Search – N.Y.

Conflict of Interest: This paper has been presented at the ICENTE'21 (5th International Conference on Engineering Technologies) held in Konya (Turkey), November 18-20, 2021.) and recommended being submitted to OJN as a selected paper.

Financial Disclosure: This work was supported by The Scientific and Technical Research Council of Turkey (TÜBİTAK) with grant number 120M717 and the Office of Scientific Research Projects of Karadeniz Technical University, Turkey, with the grant number FBA-2020-8974.

References

[1] Kruth JP, Leu MC, Nakagawa T. Progress in additive manufacturing and rapid prototyping. CIRP Ann - Manuf Technol. 1998;47:525–540.

[2] Attaran M. The rise of 3-D printing: The advantages of additive manufacturing over traditional manufacturing. Bus Horiz. 2017;60:677

[3] Wout De Backer. Multi-Axis Multi-Material Fused Filament Fabrication with Continuous Fiber Reinforcement by Wout De Backer Bachelor of Science Delft University of Technology 2011 Master of Science Delft University of Technology 2013 Submitted in Partial Fulfillment of th. 2017;

[4] Ngo TD, Kashani A, Imbalzano G, et al. Additive manufacturing (3D printing): A review of materials, methods, applications and challenges. Compos Part B Eng. 2018;143:172–196.

[5] Spoerk M, Arbeiter F, Cajner H, et al. Parametric optimization of intra- and inter-layer strengths in parts produced by extrusion-based additive manufacturing of poly(lactic acid). J Appl Polym Sci. 2017;134:1–15.

[6] Coogan TJ, Kazmer DO. Bond and part strength in fused deposition modeling. Rapid Prototyp J. 2017;23:414–422

[7] Krajangsawasdi N, Blok LG, Hamerton I, et al. Fused deposition modelling of fibre reinforced polymer composites: A parametric review. J Compos Sci. 2021;5.

[8] Yan M, Tian X, Peng G, et al. High temperature rheological behavior and sintering kinetics of CF/PEEK composites during selective laser sintering. Compos Sci Technol. 2018;165:140–147.

[9] Williams DF, McNamara A, Turner RM. Potential of polyetheretherketone (PEEK) and carbon-fibre-reinforced PEEK in medical applications. J Mater Sci Lett. 1987;6:188–190.

[10] Ravi AK, Deshpande A, Hsu KH. An in-process laser localized pre-deposition heating approach to inter-layer bond strengthening in extrusion based polymer additive manufacturing. J Manuf Process. 2016;24:179–185.

[11] Shaffer S, Yang K, Vargas J, et al. On reducing anisotropy in 3D printed polymers via ionizing radiation. Polymer (Guildf). 2014;55:5969–5979.

[12] Du J, Wei Z, Wang X, et al. An improved fused deposition modeling process for forming large-size thin-walled parts. J Mater Process Technol. 2016;234:332–341.

[13] Günay M, Gündüz S, Yılmaz H, et al. PLA Esaslı Numunelerde Çekme Dayanımı İçin 3D Baskı İşlem Parametrelerinin Optimizasyonu. J Polytech. 2019;0900:73–79.

[14] Ning F, Cong W, Hu Y, et al. Additive manufacturing of carbon fiber-reinforced plastic composites using fused deposition modeling: Effects of process parameters on tensile properties. J Compos Mater. 2017;51:451–462.

[15] Jo W, Kwon OC, Moon MW. Investigation of influence of heat treatment on mechanical strength of FDM printed 3D objects. Rapid Prototyp J. 2018;24:637–644.

[16] Nakagawa Y, Mori Kichiro, Maeno T. 3D printing of carbon fibre-reinforced plastic parts. Int J Adv Manuf Technol. 2017;91:2811–2817.

[17] Caminero MA, Chacón JM, García-Moreno I et al. Interlaminar bonding performance of 3D printed continuous fibre reinforced thermoplastic composites using fused deposition modelling.

Polym Test. 2018;68:415–423.

[18] Matsuzaki R, Ueda M, Namiki M, et al. Three-dimensional printing of continuous-fiber composites by in-nozzle impregnation. Sci Rep. 2016;6:1–7.

[19] Iragi M, Pascual-González C, Esnaola A, et al. Ply and interlaminar behaviours of 3D printed continuous carbon fibre-reinforced thermoplastic laminates; effects of processing conditions and microstructure. Addit Manuf. 2019;30:100884.

[20] R. Gümrük And A. Uşun, "Additive Manufacturing of Continuous Fiber-Reinforced Composites with High Mechanical Properties From PLA Thermoplastic Resin by Fused Deposition Method," TICMET'20, Gaziantep, Turkey, pp.196-203, 2020

Open Journal of Nano
ISSN: 2147-0081
(2022) 7–1
Research Article / Araştırma Makalesi

Investigation of the Use of Marble Powder in Production of High Strength Concretes

*[1]Tuba Demir, [1]Kürşat Esat Alyamaç

[1]Fırat University-Civil Engineering Depart., Elazıg, Turkey.
*Corresponding author, e-mail: t.demir@firat.edu.tr, Tel: 0 424 237 4262

Submission Date: 09.12.2021 Acceptation Date: 17.01.2022

Abstract - The first of the aims of this study is to determine the amount of marble powder to be used in the optimum amount for high strength concrete (YDB). The second is to contribute to reducing the use of natural resources by using marble powder from waste materials in the production of YDB. For this purpose, marble powder was used by replacing it with fine aggregate at 0-8-16-24% by weight. In order to increase the pozzolanic activity in concrete mixtures and to ensure maximum use of marble powder, silica fume has been used by replacing it with cement at 10% by weight. The slump test was applied to the obtained mixtures. Then f_c-7., f_c-28. and f_c-90. days, it was kept in the curing pool to be subjected to the compressive strength test. According to the results obtained from the compressive strength test, the optimum amount of marble powder was determined by taking into account the high strength value. In addition, it is thought that the use of marble powder contributes positively to the compressive strength of concrete, consumption of natural resources and reduction of environmental pollution.

Keywords: High strength concrete, marble powder, compressive strength, silica fume

Yüksek Dayanımlı Beton Üretiminde Mermer Tozu Kullanımının Araştırılması

Öz - Bu çalışmanın amaçlarından birincisi, yüksek dayanımlı betonlar (YDB) için optimum miktarda kullanılacak mermer tozu miktarının belirlenmesidir. İkincisi, YDB üretiminde atık malzemelerden mermer tozu kullanarak doğal kaynakların kullanımının azaltılmasına katkı sağlamaktır. Bunun için ince agrega mermer tozu ile ağılıkça %0, %8, %16 ve %24 oranlarında yer değiştirilerek kullanılmıştır. Beton karışımlarda puzolanik aktiviteyi arttırmak ve mermer tozunun maksimum kullanımını sağlamak için çimentonun ağırlıkça %10'u kadar silis dumanı ilave edilmiştir. Elde edilen karışımlara slump deneyi uygulanmıştır. Daha sonra f_c-7., f_c-28. ve f_c-90. günlerde basınç dayanımı testine tabi tutulmak üzere kür havuzunda bekletilmiştir. Basınç dayanımı testinden alınan sonuçlara göre optimum mermer tozu miktarı, yüksek dayanım değeri dikkate alınarak belirlenmiştir. Ayrıca mermer tozu kullanımının, beton basınç dayanımına, doğal kaynak tüketimine ve çevre kirliliğinin azaltılmasına olumlu yönde katkı sağladığı düşünülmüştür.

Anahtar kelimeler: Yüksek dayanımlı beton, mermer tozu, basınç dayanımı, silis dumanı

Graphical Abstract

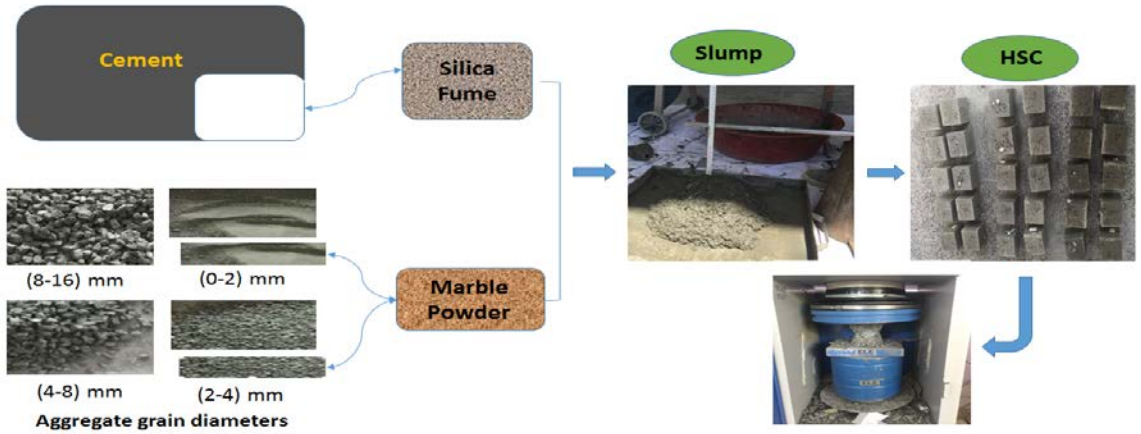

Open Journal of Nano
ISSN: 2147-0081
(2022) 7–1
Research Article / Araştırma Makalesi

1. Introduction

Concrete produced with traditional materials leads to the reduction of available natural materials. In recent studies, approaches have been developed to include waste materials as an alternative to traditional methods in concrete production [1]. With the use of these waste materials, the negative effects on the environment are reduced, environmental efficiency is increased and solutions are found for the storage problems of wastes. Marble powder and silica fume are widely used in sustainable concrete mixes [2].

Aggregates constitute approximately 70% of the concrete volume [3]. These aggregates are obtained from natural sources such as quarries or seabeds [4]. The increase in concrete production day by day causes the consumption of these natural resources and the emergence of environmental problems. In order to eliminate this problem, it is used in concrete production by replacing waste materials with aggregate [5]. One of these waste materials is marble powder.

Marble powder comes out during the cutting process of marble stones and blocks. It does not have a pozzolanic feature, but by creating a filling effect in concrete mixtures, it provides more void-free concrete [6]. Thus, it affects the compressive strength of concrete positively. On the other hand, due to the small specific surface area of the marble powder, the concrete increases the water requirement. Therefore, the use of more than the optimum amount in concrete mixtures reduces the compressive strength [7]. Environmental benefits are also obtained by using marble powder in concrete mixtures [8]. The use of waste in concrete production provides many advantages. Because the accumulation of industrial wastes such as marble powder, silica fume, fly ash, slag also creates ecological problems, which creates environmental concerns with the occupation of lands [9]. The storage of these wastes, which are formed in large volumes, causes a lot of damage to the environment and living things in these areas [10]. Therefore, the safe use of these wastes is also of great importance for sustainability [11]. Also, by replacing these additives with cement or aggregate in certain proportions, the amount of cement and aggregates is reduced and enables more environmentally friendly concrete production [12]. In current studies, cement and silica fume have been replaced by cement between 5% and 20% on average. In the experimental studies, it has been observed that the use of silica fume above these rates causes a decrease in the compressive strength of the concrete. marble powder was replaced with fine aggregate.

In this study, it was aimed to determine the amount of marble powder to be used in the optimum amount for high strength concrete (YDB). In the literature, the optimum ratio of marble powder to be used in the YDB is not specified. Therefore, in this study, it is anticipated to contribute to the literature by determining this rate. In addition, it is thought that the use of marble powder in the production of YDB will contribute to the reduction of natural resource consumption, as well as gains in terms of works that require great labor and cost such as obtaining fine aggregate and transportation (Figure 1). For this purpose, fine aggregate was used by replacing marble powder at the rates of 0%, 8%, 16% and 24% by weight. In order to increase the pozzolanic activity in concrete mixes and to ensure the maximum use of marble dust, silica fume was added up to 10% by weight of the cement. The slump test was applied to the obtained mixtures. Then fc-7., fc-28. and fc-90. days, it was kept in the curing pool to be subjected to the compressive strength test. According to the results obtained from the compressive strength test, the optimum amount of marble dust was determined by taking into account the high strength value.

Open Journal of Nano
ISSN: 2147-0081
(2022) 7–1
Research Article / Araştırma Makalesi

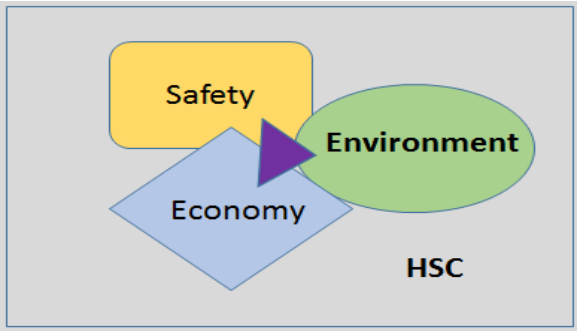

Figure 1. The key elements of the HSC

2. Materials and Methods

2.1. Materials

In this study, CEM I 42.5 R portland cement type produced in accordance with TS EN 197-1 standard was used [13]. Marble powder was used by replacing 0%, 8%, 16% and 24% fine aggregate. In order to increase the pozzolanic activity and to ensure the maximum use of marble powder, 10% by weight of silica fume was added to the cement. The physical and chemical properties of these materials are given in Table 1.

Table 1. Chemical and physical properties (%) of materials used in HSC

Chemical Properties	Cement (C)	Silica Fume (SF)	Marble Powder (MP)
CaO	63.19	0.40	40.45
SiO_2	19.07	94.10	28.35
Fe_2O_3	3.72	1.50	9.70
Al_2O_3	4.82	0.90	0.17
SiO_3	2.94	94.10	0.02
Na_2O	0.39	0.40	0.05
K_2O	0.62	0.90	0.01
MgO	1.83	0.10	16.25
Cl	0.0101	-	-
Insoluble residue	0.56	-	-
Loss of ignition	3.43	-	4.84
Physical Properties			
Specific surface cm^2/g	3838		3920
Specific gravity g/cm^3	3.13	2.20	2.71
Initial setting time (min)	135	-	-
Final setting time(min)	215	-	-
Total volume exp. (mm)	1	-	-

In the study, andesite aggregate, which has a high compactness, was used. This type of aggregate is dark colored, non-absorbent, non-dispersible and highly compact. At the same time, andesite aggregate contains 52-63% quartz [10,11]. The maximum aggregate grain diameter (Dmax) used in experimental studies is 16 mm. Aggregates are divided into 4 different groups as 0-2, 2-4, 4-8, 8-16 mm. Aggregates separated by sieve classes are given in Figure 2. The grain density values of the aggregate and usage rates in the mixture are presented in Table 2.

Open Journal of Nano
ISSN: 2147-0081
(2022) 7–1
Research Article / Araştırma Makalesi

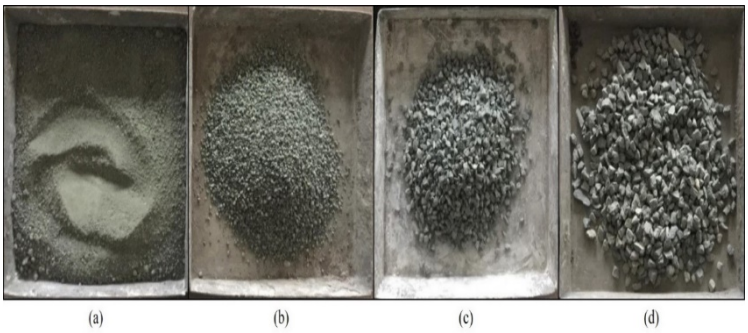

Figure 2. Aggregate grain diameters a) (0-2) mm, b) (2-4) mm, c) (4-8) mm, d) (8-16) mm

Table 3. The grain density values of the aggregate and usage rates in the mixture

Aggregate Group	Specific Gravity (gr/cm^3)	Mixture Rate (%)
0-2 mm	2.74	30
2-4 mm	2.71	20
4-8 mm	2.69	20
8-16 mm	2.69	30

2.2. Preparation of Samples

In the experiments, 4 series of concrete mixtures with different mixing ratios were prepared. Cement dosage was taken as 500 kg/m3 and water/binder ratio was 0.30 in the mixtures. Marble powder was used by replacing 0%, 8%, 16% and 24% fine aggregate. Silica fume was used as a mineral additive by replacing 10% by weight with cement. Due to the high water absorption properties of the materials used, Optima 280 SC3 chemical additive was used at the rate of 1.4% by weight of the cement to provide a fluid consistency in the concrete. The density value of this additive material is 1.08 gr/cm^3 and its ph value is 6. The coding and ratios of these samples are presented in Table 3.

Table 3. Proportions of the concrete mixtures (kg/m^3)

Mix Code	Cement	Water	Silica Fume	(0-2) mm	(2-4) mm	(4-8) mm	(8-16) mm	Chemical Additive
S500-1	475	150	35.1	545	359	358	535	6.65
S500-2	475	150	35.1	523	345	358	535	6.65
S500-3	475	150	35.1	501	330	358	535	6.65
S500-4	475	150	35.1	480	316	358	535	6.65

The slump test, which is one of the fresh concrete tests, was applied to the concrete mixtures in the first stage. Afterwards, the prepared concrete mixture was placed in molds of 100x100x100 mm. The samples, which were cured by waiting in the laboratory environment for 24 hours, were removed from the molds and left in the curing pool. In order to determine the hardened concrete properties, the samples were subjected to standard compressive strength tests on the 7th, 28th and 90th days.

3. Conclusions and Evaluation

3.1.Fresh concrete properties

Slump values of 4 series mixtures produced in the experimental study were determined. The numerical results of these slump values are compared by showing them as graphics (Figure 3).

Open Journal of Nano
ISSN: 2147-0081
(2022) 7–1
Research Article / Araştırma Makalesi

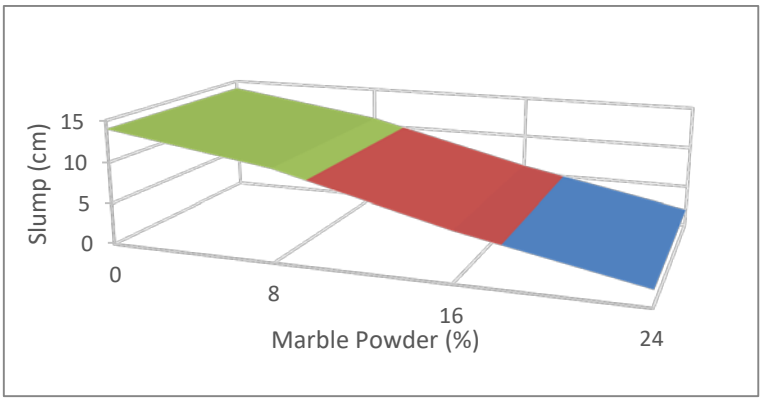

Figure 2. Comparison of slump values of the series

When Figure 3 is examined, it is observed that the slump value decreases with the increase in the amount of marble powder. As stated in the literature, marble powder, which creates a filling effect in concrete mixtures, also increases the water requirement of the concrete mixture due to its thinness.

3.2.Compressive Strength

In this study, it is aimed to determine the amount of marble powder to be used in the optimum amount for HSC based on the compressive strength. For this, 4 series of concrete mixes were prepared and f_c-7., f_c-28. and f_c-90. Compressive strength test was applied. The numerical results of the S500 dosed sample groups are shown in Figure 3 as graphics.

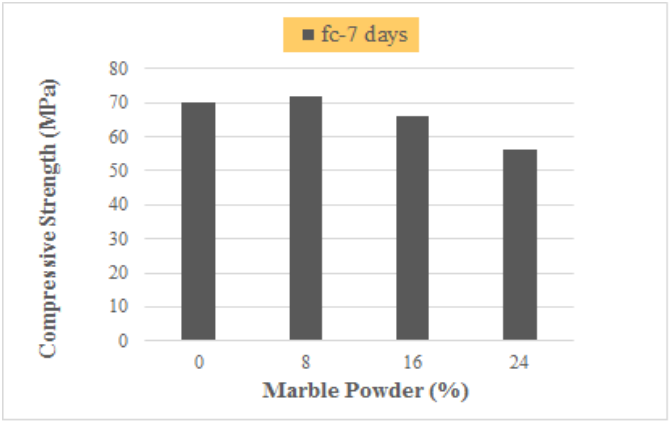

(a)

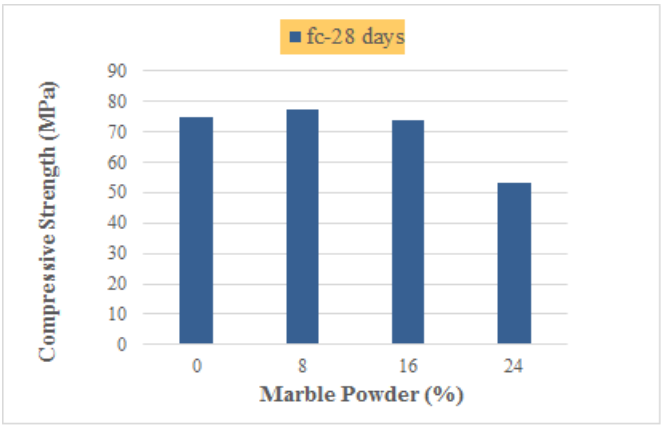

(b)

Open Journal of Nano
ISSN: 2147-0081
(2022) 7–1
Research Article / Araştırma Makalesi

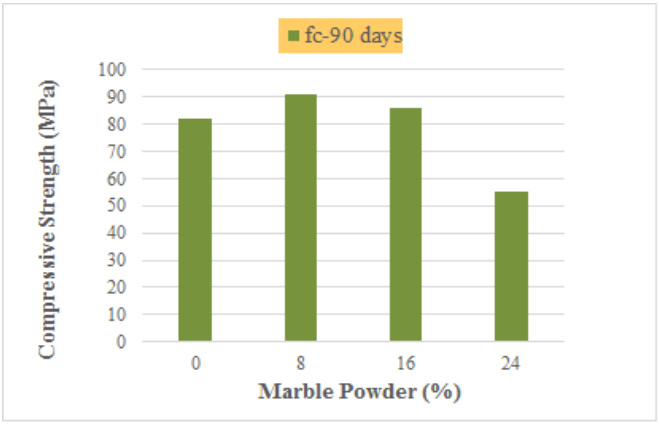

(c)

Figure 3. (a) f_c-7 days compressive strength values (b) f_c-28 days compressive strength values (c) f_c-90 days compressive strength values

When Figure 3 is examined in terms of compressive strength, the compressive strength value was found to be high in the series in which 8% of marble powder was used in general. Due to the filling effect of the marble powder, the compressive strength value in the 1st series, in which marble powder is not used, was lower than in the 2nd series. On the other hand, due to the low machinability of the 3rd and 4th series in which marble powder is used at 16% and 24%, it is thought that the compressive strength of the materials used in the mixture cannot be homogeneously mixed and lumped and placed in the molds well [16]. Therefore, as a result of the data obtained from the experiments, it was seen that the optimum amount of marble powder for HSC was 8%.

The use of more than optimum amount of marble powder complicates the mixing, placing and compaction of concrete due to the increasing water demand. This adversely affects the compressive strength [17]. On the other hand, it is thought that the use of marble powder in HSC mixtures will contribute to the environment and economy.

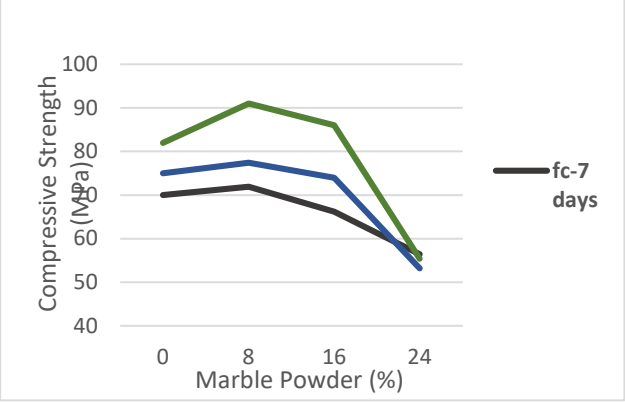

Figure 4. Comparison of f_c-7, f_c-28, and f_c-90 days compressive strength values

Figure 4 shows the comparison of f_c-7, f_c-28, and f_c-90 daily compressive strength values of all series. When the graph is examined, when the increase in compressive strength of f_c-7 and f_c-28 days is compared with the increase in compressive strength of fc-28 and fc-90; The increase after f_c-28 days was greater. The reason for this increase is the addition of silica fume with high pozzolanic activity to the mixture [18]. In parallel with the literature, it is seen that silica fume in concrete mixtures shows a great increase in strength at advanced age and final age values [19]. Likewise, it is clearly seen that the highest value in the compressive strengths of marble powder on the 7th, 28th and 90th days is 8%.

4. Conclusions

In this study, the amount of marble powder that can be used at the optimum rate in HSCs was determined and its effect on the performance of concrete was compared. For the study, 4 series of concrete mixes were prepared. Series slump experiments with f_c-7, f_c-28 and f_c-90. Compressive strength tests were carried out. The data obtained and the variation of the marble powder ratio were compared. The general results of the study are given below:

• Since proper workability could not be achieved in concrete mixtures with high marble powder content, a decrease in the compressive strength value was observed.

• It has been determined that high strength is obtained with the use of optimum marble powder and silica fume.

• From the data obtained as a result of the experiments, it was observed that the pozzolanic activity of the silica fume continued for a long time.

As a result of the experiments, the optimum marble powder ratio was determined. In future studies, it is planned to make trial mixtures for HSC at different dosage values at intervals where the marble powder is 8% +/-2%. As a result of the study, it is aimed to produce more environmentally friendly concrete.

Peer-review: Externally peer - reviewed.

Author contributions: Concept – T.D., K.E.A.; Data Collection &/or Processing - T.D., K.E.A; Literature Search - T.D.; Writing - T.D.

Conflict of Interest: This paper has been presented at the ICENTE'21 (International Conference on Engineering Technologies) held in Konya (Turkey), November 18-20, 2021.)

Financial Disclosure: The authors declared that this study has received no financial support.

References

[1] R. Zhong, K. Wille, and R. Viegas, “Material efficiency in the design of UHPC paste from a life cycle point of view,” *Constr. Build. Mater.*, vol. 160, 2018.

[2] S. Abbas, A. M. Soliman, and M. L. Nehdi, “Exploring mechanical and durability properties of ultra-high performance concrete incorporating various steel fiber lengths and dosages,” *Constr. Build. Mater.*, 2015.

[3] R. B. Ardalan, Z. N. Emamzadeh, H. Rasekh, A. Joshaghani, and B. Samali, “Physical and mechanical properties of polymer modified self-compacting concrete (SCC) using natural and recycled aggregates,” *J. Sustain. Cem. Mater.*, vol. 9, no. 1, pp. 1–16, 2020.

[4] N. Tošić, S. Marinković, T. Dašić, and M. Stanić, “Multicriteria optimization of natural and recycled aggregate concrete for structural use,” *J. Clean. Prod.*, vol. 87, pp. 766–776, 2015.

[5] D. Y. Osei and E. N. Jackson, “Compressive Strength of Concrete Using Sawdust as Aggregate,” *Int. J. Sci. Eng. Res.*, vol. 7, no. 4, pp. 1349–1353, 2016.

[6] D. K. Ashish, “Concrete made with waste marble powder and supplementary cementitious material for sustainable development,” *J. Clean. Prod.*, vol. 211, pp. 716–729, 2019.

[7] K. E. Alyamac, E. Ghafari, and R. Ince, “Development of eco-efficient self-compacting concrete with waste marble powder using the response surface method,” *J. Clean. Prod.*, vol. 144, pp. 192–202, 2017.

[8] K. E. Alyamac and A. B. Aydin, “Concrete properties containing fine aggregate marble

powder," *KSCE J. Civ. Eng.*, vol. 19, no. 7, pp. 2208–2216, 2015.

[9] A. A. Thakare, A. Singh, V. Gupta, S. Siddique, and S. Chaudhary, "Sustainable development of self-compacting cementitious mixes using waste originated fibers: A review," *Resour. Conserv. Recycl.*, p. 105250, 2020.

[10] R. Kumar, S. Singh, and L. P. Singh, "Studies on enhanced thermally stable high strength concrete incorporating silica nanoparticles," *Constr. Build. Mater.*, vol. 153, pp. 506–513, 2017.

[11] J. Wang, Y. Wang, Y. Sun, D. D. Tingley, and Y. Zhang, "Life cycle sustainability assessment of fly ash concrete structures," *Renew. Sustain. Energy Rev.*, vol. 80, pp. 1162–1174, 2017.

[12] A. Drammeh and O. Sidibeh, "Trends and Developments in Green Cement and Concrete Technology," in *2015-Sustainable Industrial Processing Summit*, 2015, vol. 6, pp. 79–80.

[13] P. and C. C. Cement - Part 1: General Cements, Composition, "TS EN 197-1," Turkey, 2012.

[14] O. Soykan, Ö. Cengiz, and Ö. Cenk, "Investigation of the Usability of Slate and Andesite as Concrete Aggregate," *J. Suleyman Demirel Univ. Grad. Sch. Nat. Appl. Sci.*, vol. 19, no. 1, 2015.

[15] A. D. Öcal and M. Dal, "Decays in natural stones," *Archit. Found. Econ. Enterp. Istanbul*, 2012.

[16] N. M. Azmee and N. Shafiq, "Ultra-high performance concrete: From fundamental to applications," *Case Stud. Constr. Mater.*, vol. 9, 2018.

[17] V. Singhal, R. Nagar, and V. Agrawal, "Use of marble slurry powder and fly ash to obtain sustainable concrete," *Mater. Today Proc.*, vol. 44, pp. 4387–4392, 2021.

[18] S. Chithra, S. R. R. Senthil Kumar, and K. Chinnaraju, "The effect of Colloidal Nano-silica on workability, mechanical and durability properties of High Performance Concrete with Copper slag as partial fine aggregate," *Constr. Build. Mater.*, vol. 113, 2016.

[19] S. A. Khedr and M. N. Abou-Zeid, "Characteristics of silica-fume concrete," *J. Mater. Civ. Eng.*, vol. 6, no. 3, pp. 357–375, 1994.

Open Journal of Nano
ISSN: 2147-0081
(2022) 7-1
Research Article

Determination of Metal Content and Biological Activities of Radish Plant Consumed as Turnip by Public in Siirt Region

[*1] İbrahim Tegin, [2] Bülent Hallaç, [1] Hasan Özden, [3] Mehmet Fidan

[1]Siirt University, Faculty of Arts and Science, Department of Chemistry, Siirt, Turkey,
[2]Siirt University, Faculty of Engineering and Architecture, Department of Food Engineering, Siirt, Turkey,
[3]Siirt University, Faculty of Arts and Science, Department of Biology, Siirt, Turkey
* Corresponding author, e-mail: ibrahim.tegin@gmail.com

Submission Date: 13.12.2021 Acceptation Date: 19.01.2022

Abstract - This study was carried out on turnip (avtitu) obtained from a radish ecotype grown in Eruh region of Siirt. Antioxidant capacities, total phenolic and flavonoid amounts of DPPH (free radical scavenging), Ferric ion reducing antioxidant power (FRAP) analyses were performed in extracts obtained from radish with different solvents. In addition, the metal content of the samples and the elemental analysis of the soil samples taken in the area where they were collected were made. In this study, the content of total phenolic, total flavonoid, DPPH highest % inhibition values and the highest values of the ferric ion reducing antioxidant power (FRAP) were 71.97 ± 14.54 mg / mL Gallic acid equivalents, 298.17 ± 12.81 mg / mL routine equivalent, 66.88% and 3.29 ± 0.01 mg / mL $FeSO_4$ equivalents were detected in the above-ground fractions methanol extract, respectively. Samples of the turnip beverage traditionally produced by the people from the Eruh region of Siirt were randomly obtained from eleven families. Some physicochemical tests such as pH, water activity, Oxidation-Reduction (O / R; Eh) Potential Value, colour analysis, dry matter content and % salt ratio and microbiological tests such as TMAB, yeast, mould, Staphylococcus species, Lactobacillus spp., coliform group bacteria and E. coli were applied to these avtitu samples.

Keywords: Antioxidant, radish, microbiological quality, DPPH, FRAP, Siirt

Siirt Yöresinde Halk Tarafından Şalgam Olarak Tüketilen Turp Bitkisinin Metal İçeriği Ve Biyolojik Aktivitelerinin Belirlenmesi

Öz - Bu çalışma, Siirt'in Eruh bölgesinde yetiştirilen bir turp ekotipinden elde edilen şalgam (avtitu) üzerine yapılmıştır. Turptan farklı çözgenler ile elde edilen ekstraklarda antioksidan kapasiteleri, toplam fenolik ve flavonoid miktarları DPPH (serbest radikal süpürme), Ferrik iyon indirgeyici antioksidan gücü (FRAP) analizleri yapılmıştır. Ayrıca örneklerin metal içeriği ve toplandığı alanda alınan toprak numunelerinin element analizi yapılmıştır. Çalışma sonucunda toplam fenolik madde miktarı en yüksek değer 71,97±14,54 mg/mL Gallik asit eşdeğeri ile toprak üstü kısımların metanol ekstraktında tespit edilmiştir. Toplam flavonoid en yüksek değer 298,17±128,13 mg/mL rutin eşdeğeri ile toprak üstü kısımlarına ait metanol ekstraktında tespit edilmiştir. DPPH en yüksek % inhibisyon değeri %66,88 ile turp örneklerinin torak üstü kısmında metanol ekstraktında tespit edilmiştir. Ferrik iyon indirgeyici antioksidan gücü (FRAP) en yüksek değer 3,29±0,01 mg/mL FeSO4 eşdeğeri olarak toprak üstü kısımlara ait metanol ekstraktında tespit edilmiştir. Element içeriği Kalsiyum, Potasyum ve Sodyum gibi besin açısından önemli olan elementler açısından zengin bulunmuştur. Toprak Analizi bakımından bakıldığında organik madde oranı iyi, alınabilir fosfor çok fazla ve alınabililir potasyum iyi olarak tespit edilmiştir.

Anahtar kelimeler: Antioksidant, turp, DPPH, FRAP, Siirt

Open Journal of Nano
ISSN: 2147-0081
(2022) 7–1
Research Article

1. Introduction

Radish (*Raphanus sativus* L.) belongs to the Brassicaceae (Cruciferae) family and has a wide variation, spreading area and production especially in China, Japan, Korea and South Asia, and it is a rich nutrient-rich vegetable that has an important place in meeting the fresh vegetable needs of people. Many plants, both naturally grown and cultivated in Turkey, are used by the public against many diseases due to their functional structure.

Most of the radish production in our country is carried out in Kadirli district of Osmaniye province. The most grown types are black (bayır), red, white, Chinese and Japanese radish. The public against many diseases due to their functional structure uses many plants, both naturally grown and cultivated in Turkey. One of the plants that be considered as a functional food is radish.

It is known that the production of fermented foods is as old as human history and they are generally produced traditionally [1]. Fermented foods are among the most consumed products in daily life. It is known that fermented foods such as yoghurt, cheese and pickles are longer lasting and more beneficial than the raw materials used [2].

In addition to the prolongation of the storage period of the obtained products, new products can be obtained and various vitamins and organic acids can also be obtained [3].

Microorganisms involved in fermentation include lactic acid bacteria, propionic acid bacteria, some alcohol-producing yeasts and moulds. Acetic acid bacteria are encountered in products produced under aerobic conditions [2].

Considering the activities of microorganisms involved in fermentation, fermentation microbiology is becoming increasingly important today. Microorganisms that show some functional properties that play a role in fermentation also have important positive effects on health [4],[6]. Although pickle, wine, vinegar and olives are the leading vegetable-origin fermented products, there are also various herbal fermented products known as soy sauce, tempeh, miso, ogi and gari in different regions of the world.

Avtitu is one of the products used in our city as a vegetable origin. For the fermentation of avtitu, the tuber of the plant, sourdough and salt are used as additives. It is obtained by the traditional method, depending on the amount of yeast used in fermentation at about 25 ° C, by maturing from a few days to a few weeks. The production technique of this avtitu is similar to that of turnip production. Bulgur flour (setik), water, black carrot, salt, sourdough and turnip radish are used in turnip production. In the first stage of turnip making; by adding bulgur flour, sourdough and salt, kneading is done with water and left to fermentation at 25 ° C for 3-5 days. Towards the end of the fermentation period, the mixture swells up and cracks begin to form on it. When this formation is observed, fermentation is ended, 4 times more water is added to the dough and mixed for 5-10 minutes. When the insoluble sediment sets to the bottom, filtering is done. In the second stage of turnip production; in the fermented liquid, salt, as well as previously sliced carrot and turnip radish are added. The mixture is left to ferment again at 25 ° C for about 7 days. After fermentation, turnips are kept in a cold place and consumed [7].

It is believed that the tubers of the plant known as avtitu in the province of Siirt have positive effects in terms of health by fermentation and thus it is consumed with love. This study was conducted to determine the microbiological and some physicochemical properties of avtitu drink, which is frequently consumed in Siirt province, and to determine whether its consumption would pose a public health hazard. In this way, it is aimed for the first time in the region that this study will be a reference for future studies and to raise awareness of producers and consumers about food safety practices that may put public health at risk. It is aimed to encourage the production of this product in more hygienic and modern conditions and to obtain products with high economic added value.

Open Journal of Nano
ISSN: 2147-0081
(2022) 7–1
Research Article

2. Materials and Methods

2.1. Chemicals and Instruments

The element analysis of the Radish plant samples was performed using a Perkin Elmer, Inc., Shelton, CT, USA, Model Optima TM 7000 DV ICP-OES (Inductively Coupled Plasma Optical Emission Spectrometer). Digesting of the samples was done with a Speedwave MWS-3 Berghof brand microwave oven. Salt determination of the samples was made with a salinometer. Chemicals used in this study such as HNO_3 and H_2O_2, 2,2-diphenyl-1-picrylhydrazyl (DPPH$^{\bullet}$), Folin-Ciocalteu's phenol reagent, Gallic acid and ascorbic acid were provided from Sigma Chemical Co.

2.2. Preparation of Plant Specimens for Analysis

The herbal material used in this study was obtained from Siirt-Eruh center and villages in October 2020. Radish specimens were identified by Dr Mehmet Fidan.

Plant samples dried in the shade and separated into different parts were shredded with a laboratory grinder and stored in suitable containers at +4 ^{0}C until extraction steps.

The plant samples were prepared in different ways for extraction and elemental analysis. 5 g of the ground plant samples were taken and 50 mL of distilled water, ethanol (80%) and 80% methanol were added to them. The samples were physically homogenized in a laboratory grinder for 5 minutes, then mechanically in a tissue shredder (sonicator) for 5 minutes. The samples were covered with foil and after being shaken at room temperature for 12 hours, they were centrifuged at 7500 rpm. The supernatants obtained at the end of the centrifuge were collected and the solvents were evaporated with the aid of an evaporator. By calculating the weight values of the crude extracts obtained, all samples were diluted with their solvents as 10 mg / mL. Total phenolic, total flavonoid, DPPH and FRAP analyzes of the extractions obtained in the study were performed.

2.3. Determination of total phenolic compounds

1 ml of FCR (Folin-Ciocalteu) reagent was added on plant extract and incubated for 3 minutes at room temperature. Later, 1 mL of saturated Na_2CO_3 (7%) will be added and foaming and green colour formation were expected at this stage. Then, it was incubated in the dark at room temperature for 90 minutes and absorbance at 725 nm wavelength was measured [8], [9]. Total phenolic was calculated as gallic acid equivalents ($y = 0.0823x + 0.0342$ and $R^2=0.990$).

2.4. Determination total flavonoid content

Flavonoid content is based on the study done by reading the reaction of the extracts with $NaNO_2$ and $AlCl_3$ at a wavelength of 510 nm (Park ve ark. 2008). After adding 400 µL of 80% methanol to 1 mL of extract (separate for each concentration prepared), 30 µL of 5% $NaNO_2$ was added and kept for 6 minutes. The resulting pinkish colour absorbance was read at 510 nm wavelength. The total flavonoid content was made according to the different concentrations of Rutin (0.1-1 mg / mL) and the calculation was made according to the formula $y = 0.0081 + 0.0168$ and $R^2=0.9962$, which was constructed by the rutin standard.

2.5. DPPH radical scavenging activity

DPPH solution generates a deep purple colour with maximum absorbance at 517 nm. When a solution containing antioxidant substance or substances is added to this DPPH solution, this dark purple colour starts to lose its colour over time. Colour change is accepted as the colourimetric indicator of antioxidant substances to suppress DPPH radical. The change is expressed as a percentage (%). For each concentration prepared, 1 mL of plant extracts were placed in separate tubes and 4 ml of DPPH (0.001 M DPPH, dissolved in pure methanol) solution was added and mixed thoroughly [10]. Then it was left to incubate for 30 minutes and its absorbance was measured at 517 nm in a spectrophotometer.

$$\% \text{ Inhibition} = \frac{A_{control} - A_{sample}}{A_{sample}} x100$$

Open Journal of Nano
ISSN: 2147-0081
(2022) 7–1
Research Article

Where,

$A_{control}$: The initial concentration of the DPPH

A_{sample} : The absorbance of the remaining concentration of $DPPH^{\bullet}$ in the extracts or positive controls [11].

2.6. Elemental analysis of samples

For the elemental analysis of the samples, 0.6-1.0 g of the samples weighed and solubilized with the help of a microwave. For this, the weighed samples were transferred to pressure-resistant polytetrafluoroethylene (PTFE) containers and after adding HNO_3 / H_2O_2 (10.0/2.0) acid mixture, the digesting process was carried out in the Speedwave MWS-3 Berghof brand microwave oven under the conditions specified by Uyan (2017) [13], [14]. After the necessary procedures, elemental analysis was performed with Model Optima ™ 7000 DV ICP-OES (Inductively Coupled Plasma Optical Emission Spectrometer) (Perkin Elmer, Inc., Shelton, CT, USA).

2.7. Analysis of soil

Soil samples taken from different locations were analyzed according to the method given in Table 1.

Table 1. The analysis method Soil.

Analysis method	Method	Unit
pH	Determination of pH in 1:2 Soil-Water Mixture [15]	
EC	Determination of EC in 1:5 Soil-Water Mixture	dS/m
Lime	TS EN ISO 10693 (Calcimeter Method)	%
Texture	Bouyoucos Hydrometer Method	%
Organic matter	Modified Walkley Black Age Burning Method	%
phosphorus available	TS ISO11263 [16] (Olsen ve ark., 1954) (Sodium Bicarbonate Method)	Kg/da
Potassium available	Ammonium Acetate Method	Kg/da
Calcium available	Ammonium Acetate Method	Kg/da
Magnesium available	Ammonium Acetate Method	Kg/da
Zinc	DTPA Solution Extraction Method	ppm
Manganese	DTPA Solution Extraction Method	ppm
Iron	DTPA Solution Extraction Method	ppm
Copper	DTPA Solution Extraction Method	ppm

2.8. Microbiological Analyses of Turnip Samples

In this study, avtitu samples obtained from 11 different people, approximately one liter each, from a traditionally produced radish-turnip juice (avtitu) sample in Eruh district of Siirt. Microbiological analyses were carried out to determine whether the procured avtitu samples contain potential hazards for public health.

2.9. Preparation of Dilutions

10 mL sample taken under aseptic conditions was weighed in stomacher bags in 90 mL of buffered peptone water and homogenized for 2 minutes in the stomacher device, and sterile decimal dilutions were prepared from the homogenate with sterile peptone water up to 10^{-8} [17].

To determine the yeast-mould count; PDA (Potato Dextrose Agar, Oxoid CM139) was planted with the spreading method from these dilutions instead of solid media, and then incubated at 25 ^{0}C under aerobic conditions for 72-120 hours. All colonies formed on the medium as a result of incubation were counted as yeast mould [17], [18].

Similarly, using these dilutions for TMAB number, PCA (Plate Count Agar, Oxoid CM463) was inoculated on solid media by the spread plate method and the colonies formed in incubation at 30 ^{0}C under aerobic conditions for 24-48 hours were counted [17], [19].

In determining the number of *Staphylococcus* spp.; Potassium tellurite (Potassium tellurite, Sigma-Aldrich, Merck) and Baird-Parker (Baird-Parker agar base, Merck) agar with microfiltration

sterilized egg yolk were added and seeded at appropriate dilutions by the smear plate method. Then, it was incubated under aerobic conditions for 18-24 hours at 35-37 ^{0}C.

In determining the number of Staphylococcus spp.; Potassium tellurite (Potassium tellurite, Sigma-Aldrich, Merck) and Baird-Parker (Baird-Parker agar base, Merck) agar with the addition of sterilized egg yolk sterilized by microfiltration were planted with appropriate dilutions by the spreading plate method. Afterwards, incubation was carried out at 35-37 ^{0}C for 18-24 hours under aerobic conditions. At the end of the incubation, convex colonies of 1.5-2.5 mm in diameter, black and surrounded by a transparent zone, formed on Baird-Parker agar medium, were evaluated as Staphylococcus species (by tests such as Gram staining, microscopic examination, fermentation of glucose under anaerobic-aerobic conditions) [20].

In the investigation of lactic acid bacteria, MRS (de Man, Rogosa and Sharpe broth, Merck) agar was inoculated with the smear plate method. In the next step, incubation was carried out at 37 °C for 24 hours under anaerobic conditions. At the end of the incubation, off-white, white and opaque colonies with a diameter of 2.5 mm growing on MRS agar were counted as *Lactobacillus* spp. [21], [22].

To determine the number of coliform bacteria, EMB agar was incubated for 24 hours at 37°C after inoculation with the smear plate method. Typical colonies formed at the end of incubation were evaluated as coliform bacteria, and metallic green colonies were evaluated as faecal coliform E. coli. In addition, to determine the number of E. coli, TBX Medium (Tryptone Bile X-Glucuronide, Oxoid, CM0945) was inoculated with the smear plate method and the Petri dishes were incubated aerobically at 44ºC for 18-24 hours. At the end of incubation, turquoise-coloured colonies were evaluated as E. coli [17], [18].

2.10. Physicochemical analysis of turnip samples

2.10.1. Determination of water activity

In the determination of water activity, it was performed with a device branded Novasina LabTouch®-a_w, [Lachen, Switzerland] [23]. After three repeated measurements were made for each sample, their averages were taken.

2.10.2. Determination of pH, oxidation-reduction (O / R; Eh) potential value

In the determination of these analysis values, Mettler Toledo Seven Compact ™ S220 [China] branded device was used with the method suggested by [24]. After three repeated measurements for each sample, their averages were taken.

2.10.3. Determination of Colour Analysis of Turnip Samples

Pen Color Art 1 L model Artoxy MSM, Istanbul, Turkey branded device was used to determine the colour analysis. L, a and b values were determined by taking the averages with 4 repeated measurements [25]–[27].

2.10.4. Determination of dry matter of Turnip Samples

For the determination of dry matter values, it was made with a Hanna® HI 96801 (Romania) digital refractometer device using the method suggested by Cemeroğlu [24].

2.11. Statistical Evaluation

SPSS-22 (Statistical Package For Social Sciences) program was used for the statistical evaluation of whether there is a difference and correlation between the samples by using Duncan test [28].

3. Results and Discussions

Vegetables and fruits contain many antioxidant compounds. These antioxidant compounds are abundant in seeds, leaves, flowers, roots, and bark [29]. Studies have reported that as a result of the consumption of large quantities of vegetables and fruits, the risk of developing diseases decreases, there is a significant decrease in cardiovascular diseases, cancer cases and mortality rates [30].

Open Journal of Nano
ISSN: 2147-0081
(2022) 7–1
Research Article

Preparing extracts from plants and using them as medicine. It dates back to 2700 BC. As in other countries of the world, many plants found by trial and error in our country, known as medicinal plants, are used in the treatment of diseases.

The first written record of the use of plants in food was found in excavations in Ancient Egypt. BC in Egypt. It is known that various herbs, especially mint, were used in the mummification of corpses in the year 2500. In mummification, corpses were treated with extracts obtained from the plants in question, and it was possible to keep them intact for centuries with other methods. In addition, plants are mentioned both as a source of healing and power in many scriptures [31]. The number of studies investigating the use of herbs and spices as natural antioxidant sources is increasing day by day [32], [33].

In our study, elemental analysis and extraction of water, 80% methanol and 80% ethanol solvents were made of different parts of the Siirt ecotype (whole tuber, tuber shell part, peeled form of tuber and above-ground green parts) of the Raphanus sativus species used for food in different ways by the public. Total phenolic, total flavonoid, DPPH, FRAP analyzes of these extracts were made. In addition, the analysis of the soils where the plant is grown has been made. In addition, samples of traditional fermented avtitu drink produced in Eruh district of Siirt province were taken randomly from 11 families and some physicochemical and microbiological tests were applied.

3.1. Statistical Evaluation

In the study conducted [34], it was found that in extractable fractions, according to radish types, Chinese radish is equivalent to 312.10 mg GAE / 100 Gallic acid, and Bayır radish is equivalent to 187.41 mg GAE / 100 g Gallic acid. The radish type with the lowest total phenolic content was found in hazelnut radish with 71.90 mg/ 100 g Gallic acid equivalent.

When Table 2 is examined, as a result of analysing extracts belonging to different solvents and parts of radish, the highest total phenolic substance amount was determined in the aboveground part of radish prepared with 80% methanol.

In the phenolic substance content analysis performed, it was determined that the highest phenolic substance content belonged to methanol surface extract with a value of 71.97 ± 14.54 mg / mL Gallic acid equivalent.

Table 2 Total phenolic matter analysis results.

Sample	Solvent	mg/mL Gallic acid equivalent.
Root without bark	Pure water	11.21 ±1.42
bark	Pure water	12.54 ±2.44
Root shell	Pure water	9.29 ±1.67
Above-ground part	Pure water	11.52 ±1.38
Root without bark	Methanol (80%)	7.18 ±1.10
bark	Methanol (80%)	10.39 ±0.41
Root shell	Methanol (80%)	25.35 ±3.34
Above-ground part	Methanol (80%)	71.97 ±14.54
Root without bark	Ethanol (%80)	14.84 ±0.79
bark	Ethanol (%80)	17.77 ±3.38
Root shell	Ethanol (%80)	16.91 ±6.51
Above-ground part	Ethanol (%80)	20.10 ±1.29

3.2. Total flavonoid content analysis

When Table 3 is examined, it has been determined that the total flavonoid content is similar to the phenolic substance content in the total flavonoid analysis. The total flavonoid substance amounts of extracts prepared with water and ethanol were reported as 280.58 mg / mL and 503.82 mg / mL routine equivalent, respectively [35]. In our study, the highest total flavonoid value was detected in the methanol extract of the above-ground parts of radish with 298.17 ± 128.13 mg / mL routine equivalent.

Open Journal of Nano
ISSN: 2147-0081
(2022) 7–1
Research Article

Table 3. Total flavonoid substance analysis results.

Sample	Solvent	mg/mL Routine equivalent.
Root without bark	Pure water	41.07±10.53
bark	Pure water	37.43±2.49
Root shell	Pure water	34.31±10.4
Above-ground part	Pure water	56.68±7.22
Root without bark	Methanol (80%)	25.62±4.2
bark	Methanol (80%)	44.4±11.17
Root shell	Methanol (80%)	183.37±85.66
Above-ground part	Methanol (80%)	298.17±128.13
Root without bark	Ethanol (%80)	66.09±4.21
bark	Ethanol (%80)	109.42±23.56
Root shell	Ethanol (%80)	53.61±2.48
Above-ground part	Ethanol (%80)	105.05±12.87

3.3. DPPH free radical scavenging activity

DPPH activity is a general test used to determine the antioxidant properties of plant extracts. According to the results of DPPH analysis, methanol extract belonging to the above-ground parts showed the highest value.

Teucrium polium L. subsp. DPPH% values of the extracts of polyum taxa prepared with water and ethanol were determined as 81.13±19.17-92.76±29.51, respectively [36]. Fidan et al. [35] reported that as a result of the analysis of the extracts prepared with water and ethanol of Origanum acutidens (Hand.-Mazz.) Ietsw. plant, water extract showed 77.53% inhibition and ethanol extract showed 90.69% inhibition. According to the results of this study, the highest % inhibition value was found in the methanol extract of the above-ground parts of the radish samples with 66.88%.

Table 4. Analysis results of DPPH %.

Sample	Solvent	DPPH %
Root without bark	Pure water	14.45
bark	Pure water	18.95
Root shell	Pure water	9.15
Above-ground part	Pure water	12.87
Root without bark	Methanol (80%)	9.91
bark	Methanol (80%)	13.58
Root shell	Methanol (80%)	38.22
Above-ground part	Methanol (80%)	66.88
Root without bark	Ethanol (%80)	14.94
bark	Ethanol (%80)	21.82
Root shell	Ethanol (%80)	9.69
Above-ground part	Ethanol (%80)	24.94

3.4. FRAP analysis

DPPH activity is a general test used to determine the antioxidant properties of plant extracts. According to the results of DPPH analysis, methanol extract belonging to the above-ground parts showed the highest value.

Open Journal of Nano
ISSN: 2147-0081
(2022) 7–1
Research Article

Table 5. The results of FRAP

Sample	Solvent	mg/mL $FeSO_4$ equivalent.
Root without bark	Pure water	1.89 ±0.03
bark	Pure water	1.98 ±0.02
Root shell	Pure water	1.59 ±0.03
Above-ground part	Pure water	2.22 ±0.04
Root without bark	Methanol (80%)	1.24 ±0.03
bark	Methanol (80%)	1.88 ±0.04
Root shell	Methanol (80%)	2.95 ±0.13
Above-ground part	Methanol (80%)	3.29 ±0.01
Root without bark	Ethanol (%80)	1.58 ±0.06
bark	Ethanol (%80)	2.52 ±0.06
Root shell	Ethanol (%80)	1.17 ±0.01
Above-ground part	Ethanol (%80)	2.4 ±0.1

When the values obtained in this study are examined, it is seen that the highest value is in the methanol extracts of the above-ground parts of radish as 3.29 ± 0.01 $FeSO_4$ equivalent. [37], as a result of the analysis of the extracts of the radish plant, reported that there is a ferric ion-reducing antioxidant potential in the equivalent of 3.56 µg / mL Gallic acid.

3.5. Elemental analysis of different parts of the radish sample

Some of the healing properties of plants come from the trace elements found in their structures [35], [38]. Excessive amounts of micronutrients or heavy metals may cause some basic problems to occur. Therefore, the determination of the properties of the chemical ingredients of the plants and their use accordingly is an important element [35], [39].

Elemental analysis of the samples were performed with the ICP-OES device. As can be seen from Table 6 the heavy metal contents of the samples are among acceptable values. Radish is rich in nutritionally important elements such as Calcium, Potassium and Sodium.

Table 6. Elemental analysis of different parts of the radish sample by ICP-OES

	Sample inner part (ppm)		Sample shell part (ppm)		All sample (Shell + inner) (ppm)	
Element	**Mean**	**sd**	**Mean**	**sd**	**Mean**	**sd**
B	14.23	0.05	16.12	0.06	20.17	0.07
Ba	14.58	0.06	15.19	0.05	14.16	0.06
Bi	3.97	0.15	4.11	0.21	3.53	0.06
Cd	0.71	0.01	0.70	0.01	0.60	0.01
Co	1.35	0.02	1.73	0.02	1.08	0.02
Cr	0.14	0.00	1.24	0.00	0.25	0.01
Cu	3.69	0.03	5.19	0.01	3.69	0.06
Fe	20.79	0.22	288.70	4.36	77.15	0.89
Li	2.15	0.02	2.82	0.02	2.00	0.01
Mn	13.62	0.21	26.56	0.35	13.91	0.10
Ni	0.99	0.01	2.59	0.07	1.54	0.04
Pb	4.69	0.12	5.02	0.30	2.82	0.07
Sr	59.98	0.19	62.96	0.48	57.33	0.05
Zn	34.24	0.13	64.11	0.06	33.50	0.01
Element	**Sample inner part (mg/g)**		**Sample shell part (mg/g)**		**All sample (Shell + inner) (mg/g)**	
	Mean	**sd**	**Mean**	**sd**	**Mean**	**sd**
Ca	9.96	0.02	10.54	0.07	10.56	0.00
K	51.22	0.33	51.47	0.25	45.33	0.19
Mg	2.29	0.00	2.39	0.00	1.57	0.02
Na	2.83	0.01	1.66	0.02	0.28	0.01

When Table 6 is examined, it has been found that Ca, K, Mg and Na values are at the level of mg, especially the amount of Fe in the shell is above 200 ppm. It has been observed that other metals accumulate more in the shell, as in Fe. The fact that the Pb amount is slightly excessive corresponds to the region where the radish sample was taken, probably where the mineral formations were located. When Sadık (2019) compared with the elemental analysis of *Eremurus spectabilis* Bieb plant, it was seen that the element values of Fe, Na, Mg, K and Ca were mg/g, whereas, in this study, the values of Ca, K, Mg and Na were at the level of mg [40].

As can be understood from this study, Ca, K, Mg and Na values were found to be much higher. Although Zn, Co and Fe (value in the crust) values are higher than Sadık (2019) values, Cu values were found to be close to each other. When compared with the oregano element analysis found in the study of Kara (2012)[41], Ca, Cd, Co, Cr (value in the crust), Sr and Zn values were lower than this study, and Ba, Cu, Fe and Mn values were found to be higher. Mg and Ni values were found close to each other.

Calcium is an imperative mineral for the ordinary working of the human body and plays a key part within the electrophysiology of cardiac tissue [42]. K takes an interest effectively within the upkeep of cardiac cadence [43].

3.6. Soil analysis

Soil samples were taken from the localities where the samples that made up the study material were grown, using appropriate methods, and subjected to different analysis methods. The results obtained are given in Table 7. According to the results of the analysis, the soils from which the study samples were taken were determined to be neutral in pH, salt-free in terms of electrical conductivity, very calcareous in terms of lime, clay in the body, good organic matter, high amount of absorbable phosphorus and good potassium.

Table 7. The results of soil analysis.

Analysis	Method	Unit	Analysis results	Evaluation result
pH	Determination of pH in 1:2 Soil-Water Mixture [15]		6.95	Neutral
EC	Determination of EC in 1:5 Soil-Water Mixture	dS/m	0.18	Saltless
Lime	TS EN ISO 10693 (Calcimeter Method)	%	38.95	Very limy Clayey
Texture	Bouyoucos Hydrometer Method	%	Clay: 46.5 Silt: 31.6 Sand: 21.9	Clayey
Organic matter	Modified Walkley Black Age Burning Method	%	3.74	Good
phosphorus available	TS ISO11263 [16] (Olsen ve ark., 1954) (Sodium Bicarbonate Method)	Kg/da	29.75	Too much
Potassium available	Ammonium Acetate Method	Kg/da	107.99	Good
Calcium available	Ammonium Acetate Method	Kg/da	445.86	
Magnesium available	Ammonium Acetate Method	Kg/da	27.87	
Zinc	DTPA Solution Extraction Method	ppm	1.01	
Manganese	DTPA Solution Extraction Method	ppm	23.43	
Iron	DTPA Solution Extraction Method	ppm	12.64	
Copper	DTPA Solution Extraction Method	ppm	2.23	

3.7. Some physicochemical and microbiological analysis results of Avtitu samples

Some physicochemical and microbiological tests of the traditional fermented avtitu beverage produced in Eruh district of Siirt province were applied. Physicochemical analysis results and microbiological analysis results of these samples are given in Table 8 and Table 9.

Table 8. Physicochemical results of avtitu samples analysed.

Sample	pH	Dry matter	Water activity	Salt %	Colour L	Colour a	Colour b	Croma
1	4.15	2.3	0.973	2.5	27.24	0.38	-1.69	1.652
2	4.16	0.1	0.974	2.0	29.12	0.31	-1.55	1.581
3	4.02	0.1	0.956	2.0	22.51	0.46	-1.63	1.694
4	4.02	0.1	0.957	2.5	23.07	0.38	-0.94	1.014
5	3.75	0.6	0.96	3.0	27.19	0.30	-1.2	1.237
6	3.84	0.3	0.964	1.25	28.10	0.38	-1.64	1.683
7	3.98	0.1	0.963	2.5	27.24	0.34	-1.45	1.489
8	3.91	0.1	0.966	1.0	27.63	0.55	-1.68	1.768
9	3.98	1.5	0.973	2.5	28.61	0.75	-2.15	2.277
10	4.37	0.1	0.962	2.0	25.63	0.28	-1.25	1.281
11	3.97	0.1	0.960	2.0	24.74	0.32	-1.11	1.155

In terms of pH, moulds and yeasts have a wider reproductive pH range than bacteria. While bacteria generally grow in the range of 4.5-9.0 pH, it is known that some pathogens (such as *Salmonella* spp., *Staphylococcus* spp., *Listeria* spp.) do not grow at pH values below 4 [44]. In this study, pH ranging from 3.75 to 4.37 was determined at an average level of 4.01. However, in this study, it was revealed that only pH was not effective (As a matter of fact, *Staphylococcus* spp. should not have been reproduced at pH like 3.84). On the other hand, control of pathogens may be impacted depending on nutrient content, water activity, temperature and the presence of inhibitor substances [20], [44]. It was seen that the increase of O / R potential in decreasing pH value is quite important ($p < 0.01$). It was also revealed that the samples analysed statistically showed a significant difference ($p < 0.01$) in terms of pH.

When examined in terms of water activity, according to these findings, conditions were provided for bacteria to easily reproduce in an environment where yeasts and moulds could easily reproduce. The water activity value ranges from 0 to 1. As this value approaches zero, the shelf life of the food extends due to the slowdown of microorganism activities, and the closer to one, the food spoils quickly as a result of the increase in microbial activity [44].

In this study, water activity, which is between 0.956-0.974, was determined at the average level of 0.964. This value is among the values that bacteria, yeast, and moulds can easily reproduce. Therefore, it indicates that the avtitu samples analyzed may spoliaged quickly. It was determined that the increase in water activity was effective between the increase in the amount of dry matter ($p < 0.05$), the increase in the colour L value (lightening the colour) $p < 0.01$ and the decrease in the colour b value (the lightening of the blue tone) at the level of $p < 0.05$. It was determined that the analyzed samples showed significant differences ($p < 0.01$) in terms of water activity.

Dry matter in foods refers to compounds other than water, such as minerals, vitamins, protein and carbohydrates [24]. Dry matter, which is closely related to its nutritional value, is one of the most important factors for the activities of microorganisms that play a role in fermentation technology. Fermentation conditions are expected to be earlier or effective if the dry matter or nutrient content is sufficient [7]. In this study, the dry matter varying between 0.1-2.3% was found at the average level of 0.49%. Due to the low dry matter here, the desired pH as a result of fermentation suggests that other organic compounds that may be formed are not sufficiently formed. It was observed that the increase in the amount of dry matter showed a significant correlation with the increase in water activity ($p < 0.05$), on the other hand, the analyzed samples did not show a significant difference in terms of dry matter content ($p > 0.05$).

Although salt is generally used in flavouring and fermentation (around 1%) to support the growth of microorganisms, it has a protective effect on prolonging the preservation of some fermented products, as well as a lethal effect on some pathogens [45]. One of the issues to be considered in the use of salt is the use of the product according to the typical feature of the product (such as 4-10% as in pickles). The salt ratio varied between 1-3% in this study, the average level was found to be 2.11%.

Open Journal of Nano
ISSN: 2147-0081
(2022) 7–1
Research Article

In this case, it has been observed that many salt-resistant microorganisms (such as *Micrococcus*, *Staphylococcus* spp.) survive under these conditions. It was determined that the analyzed samples showed a significant difference ($p < 0.01$) in terms of the amount of salt.

The oxidation-reduction potential (O / R) value gives an idea about the aerobic-anaerobic spoilage of foods. This is one of the internal factors affecting microbial activity. While food spoilage is positive in aerobic conditions (oxidation), it is negative in anaerobic conditions (reduction) [20], [44]. In this study, this value, which ranges from +165 to +209, has an average value of 189.73. Therefore, it suggests that this product is oxidized and that the microorganisms responsible for spoilage are microorganisms of aerobic origin. Statistically, the increase in the O / R potential value showed that the decrease in the pH value was a very significant ($p < 0.01$) relationship, on the other hand, there was a very significant difference ($p < 0.01$) in terms of the O / R potential of the analyzed samples.

Colour, one of the physical properties, is one of the important quality parameters. It is one of the first physical elements perceived by consumers. It is known that the pigment substances in the food, other components used as additives to the product, as well as the compounds that are reduced by microorganisms in fermentation are effective in the formation of colour [46], [47]. Among the colour values, L (darkness-lightness; takes values between 0-100), a (greenness-redness; takes values between -175 and +175), b (blueness-yellowness; takes values between -175 and +175), chroma is found by calculating the colour saturation with the formula ($(a^2+b^2)^{1/2}$). The average values of L, a, b and chroma of the samples analyzed in this study were determined as 26.458, 0.405, -1.481 and 1.530, respectively. There is a significant correlation between the increase in the colour L value and the increase in the water activity and the increase in the colour L value (lightening of the colour) $p < 0.01$, the increase in the colour b value, the decrease in the water activity, and the increase in the chroma increase in the water activity ($p < 0.05$) was determined. It was determined that the analyzed samples showed a significant difference ($p < 0.01$) in terms of colour L, a, b and chroma values, respectively.

It is thought that the amount of dry matter used and the fermentation conditions (microorganism type-number, temperature, time) may be effective in revealing the differences in terms of colour among the samples. Microbiological analysis results of the samples are given in Table 9.

Table 9. Microbiological analysis results of avtitu samples (log10 CFU/mL).

Sample	TMAB	Yeast	Mould	Staphylococcus spp.	Lactobacillus spp.	Coliform group bacteria	E. coli
1	6.30	7.20	-	-	6.54	5.30	-
2	6.70	6.15	-	-	5.40	5.60	-
3	6.48	5.30	-	-	6.04	4.30	-
4	7.70	5.48	5	-	5.78	5.00	-
5	6.00	5.48	-	-	4.00	4.48	-
6	6.78	6.18	-	2.30	6.40	5.00	-
7	7.08	6.34	-	-	6.30	4.30	-
8	7.48	6.78	-	-	7.00	6.90	-
9	7.30	5.90	-	-	6.20	5.84	-
10	7.30	5.70	-	-	6.84	6.30	-
11	6.30	4.00	-	-	4.00	4.00	-

The total number of aerobic bacteria of the samples analyzed in terms of microbiological quality was determined as 6-7.70, average 6.85 $\log_{10}$ CFU/mL. For the expected benefit in fermented products, the number of probiotic microorganisms (the number of Lactobacillus species responsible for lactic fermentation) should be at least 7 $\log_{10}$ CFU/mL [2], [48]. According to the turnip notification [49], it has been reported that there should be at most 5 $\log_{10}$ CFU/mL TMAB count. For this reason, it has been determined that the analyzed samples do not comply with the standards. Fermentation was achieved with the effect of the Saccharomyces type yeast, which is included in the

sourdough used in the production of Avtitu fermented beverage. The number of yeast detected was 4-7.20, with an average of 5.86 $\log_{10}$ CFU/mL yeast cells. However, it was stated that there should be no mould in fermented beverages or a maximum of 20 $\log_{10}$ CFU/mL in turnips. There should be no residue (the mass settling to the bottom of the residue as yeast) at the bottom of the avtitu beverage obtained. There is a moderate correlation between the TMAB number and the increase in *Lactobacillus* species numbers ($p < 0.05$). A significant correlation was determined between yeast and water activity and lactobacilli ($p < 0.05$). There was a correlation between *Lactobacillus* spp. and TMAB, yeast, coliform group bacteria ($p < 0.05$), and a correlation ($p < 0.05$) between coliform group bacteria and *Lactobacillus* species. There was no significant difference in the presence of mould and *Staphylococcus* spp. in the analyzed samples ($p > 0.05$), but; a significant difference ($p < 0.01$) was found in terms of TMAB, yeast, *Lactobacillus* spp. and coliform group bacteria.

The presence of *Staphylococcus* species (such as *S. aureus*, *S. epidermidis*) among pathogenic microorganisms indicates that the necessary hygienic conditions cannot be provided for product production. Considering that this number may increase, it should not be forgotten that it may cause infection or intoxication [50].

The number of Lactic acid bacteria has an important effect on fermentation [51]. In this study, it varied between 4-6.84 $\log_{10}$ CFU/mL and was determined at the average level of 5.86 $\log_{10}$ CFU/mL. Although this value is acceptable for fermented products, considering the number of Coliform bacteria in the final product, this value was found to be quite high (1100 units / mL) according to the literature [49]. On the other hand, the total number of coliform group bacteria was found between 4-6.90, with an average of 5.18 $\log_{10}$ CFU/mL. This value was again found higher than the turnip juice notification. *E. coli*, which is microbiologically an indicator of faecal pollution, was not encountered in any of the samples analysed in this study. Correlation analysis of Avtitu samples is given in Table 10.

Open Journal of Nano
ISSN: 2147-0081
(2022) 7–1
Research Article

Table 10. Correlation analysis of Avtitu samples**.**

	Sample	pH	Dry matter	Water activity	O/R	Salt amount	Colour L	Colour a	Colour b	Croma	TMAB	Yeast	Mould	Staphylococcus spp	Lactobacillus spp.	Coliform group bacteria	E. coli
Samples	1.00																
pH	-0.03	1.00															
Dry matter	-0.30	0.07	1.00														
Water activity	-0.19	0.24	**0.609***	1.00													
O/R	0.06	-0.985**	-0.03	-0.17	1.00												
Salt amount	-0.23	0.01	0.39	-0.04	-0.04	1.00											
Colour L	0.02	-0.13	0.33	**0.815****	0.21	-0.12	1.00										
Colour a	0.18	-0.22	0.37	0.34	0.22	-0.14	0.19	1.00									
Colour b	0.07	0.05	-0.52	-0.674*	-0.14	0.23	-0.55	-0.762**	1.00								
Croma	-0.02	-0.08	0.46	0.632*	0.16	-0.24	0.53	0.818**	-0.994**	1.00							
TMAB	0.30	0.26	-0.26	0.01	-0.35	-0.29	-0.04	0.39	-0.06	0.12	1.00						
Yeast	-0.45	0.12	0.46	**0.608***	-0.11	-0.16	0.56	0.21	-0.52	0.47	0.23	1.00					
Mould	-0.20	0.01	-0.18	-0.38	-0.18	0.22	-0.51	-0.06	0.53	-0.49	0.51	-0.15	1.00				
Staphyloccoccus spp	0.00	-0.34	-0.09	-0.02	0.36	-0.49	0.25	-0.06	-0.16	0.14	-0.05	0.12	-0.10	1.00			
Lactobacillus spp.	-0.05	0.41	0.15	0.28	-0.41	-0.45	0.14	0.36	-0.49	0.48	**0.624***	**0.712***	-0.03	0.17	1.00		
Coliform group bacteria	0.15	0.37	0.12	0.50	-0.36	-0.46	0.42	0.38	-0.38	0.39	0.59	0.55	-0.07	-0.07	**0.646***	1.00	
E. coli	.[a]	.a	.[a]	.[a]	.[a]	.[a]	.a	.a	.[a]	.[a]	.a	.a	.a	.a	.a	.a	.a

**. Correlation is significant at the 0.01 level (2-tailed).

*. Correlation is significant at the 0.05 level (2-tailed).

a. Cannot be computed because at least one of the variables is constant.

4. Conclusions

As primary health care. the number of people using alternative medicine accounts for almost 80% of the world's population. For this reason, analysis of materials used in alternative medicine based on different parameters becomes more and more important every day. The results obtained in the analyzes give us the opportunity to determine which components of these herbal products affect the disease factor. According to the analysis results of the radish samples used in this study. It has been determined that the above-ground green parts of the plant have the most antioxidant effect. However, only the underground part of this plant is used by the people in turnip production. It was concluded that it would be more beneficial to include the above-ground parts of the plant in turnip production. Therefore, the study results will be shared with the people of the region and it will be suggested to include the green parts of the plant in turnip production.

According to the Turkish Standards Institute's turnip juice standards no. TS 11149, in terms of TMAB, not all analysed avititu samples meet the standards. 90.90% of the samples in terms of yeast and 9.09% in terms of mould and Staphylococcus species do not comply with the standards. pH and 45.45% in terms of salt were not found suitable. In terms of TMAB. it was observed that 90.90% of the samples in terms of yeast number (according to 10^4 CFU/mL) and 9.09% of the samples in terms of mould and Staphylococcus were not produced under the standards.

Looking at the elemental analysis results. it was found that the highest value was at K with 51.22 ± 0.33 mg / g. In the study conducted by Kaymak in 2006 [52]. the highest value was found to be 288.42 mg / 100g in parallel with our K value. This parallel situation increases the accuracy of the results obtained in the study.

As a result, it was concluded that this beverage does not meet the microbiological criteria in terms of human health and that a sample contains high levels of mould and *Staphylococcus* spp. One sample may pose a health risk by consuming avtitu. When evaluated from a technological point of view, a standard production was not made due to the traditional production of the added additives other than standard productions. Therefore, the typical desired properties could not be achieved.

To eliminate such negative situations especially in terms of human health it is necessary to use raw materials with high microbiological quality, this product should be standardized and more modern and technological productions should be encouraged. Thus, especially small family businesses should be informed about the subject. In this way, both family businesses and regional economic contributions should be made.

Although it is believed to be beneficial among the public, it has been revealed that this fermented beverage is not produced under the standards. As seen in the microbiological findings obtained, the presence of pathogenic bacteria and mould as well as the high total number of bacteria suggest that serious health problems may occur if these products are consumed.

Peer-review: Externally peer - reviewed.

Author contributions: Concept, İ. T.; Data Collection &/or Processing – H.Ö., B.H, M.F.; Literature Search –H.Ö., İ.T., B.H.; Writing – İ.T., B.H, M.F.

Conflict of Interest: No conflict of interest was declared by the authors. This study was produced from the MSc thesis entitled "Determination of Metal Content, Antioxidant and Phenolic Compounds of the Extract Obtained by Different Parameters of Radish Plant Consumed by the Public as a Turnip in Siirt Region" by Hasan ÖZDEN, which was accepted in 2021.)

Financial Disclosure: The authors declared that this study has received no financial support.

References

[1] Jia - ping Lv and Li - Min Wang, 'Bioactive components in kefir and koumiss', in *Bioactive Components in Milk and Dairy Products*, Y. W. Park, Ed. 2009, pp. 251–262.

[2] F. Turantaş, 'Fermente Gıdalar', in *Gıda Mikrobiyolojisi*, 4th ed., Ünlütürk A & F. Turantaş, Ed. İzmir: Meta Basım Matbaacılık Hizmetleri, 2015, pp. 447–4733.

[3] S. Bulduk, *Gıda Teknolojisi*, 7th ed. Ankara: Detay Yayıncılık, 2013.

[4] Ayhan K & Orhan E., 'Fonksiyonel Gıdalar ve Biyoaktif Maddeler', in *Her Yönüyle Gıda*, C. S. & A. K. Durlu Özkaya F, Ed. İzmir: Sidas Medya Ltd. Şti., 2015, pp. 249–266.

[5] M. K. Tripathi and S. K. Giri, 'Probiotic functional foods: Survival of probiotics during processing and storage', *Journal of Functional Foods*, vol. 9, no. 1. Elsevier Ltd, pp. 225–241, Jul. 01, 2014, doi: 10.1016/j.jff.2014.04.030.

[6] D. Granato, G. F. Branco, F. Nazzaro, A. G. Cruz, and J. A. F. Faria, 'Functional foods and nondairy probiotic food development: Trends, concepts, and products', *Compr. Rev. Food Sci. Food Saf.*, vol. 9, no. 3, pp. 292–302, 2010, doi: 10.1111/j.1541-4337.2010.00110.x.

[7] O. Demirkol, 'Fermentasyon Teknolojisi', in *Her Yönüyle Gıda*, 1st ed., C. S. & A. K. Durlu Özkaya F, Ed. İzmir: Sidaş Medya, 2015, pp. 187–220.

[8] K. Slinkard and V. Singleton, 'Total phenol analysis: automation and comparison with manual methods', *Am. J. Enol. Vitic.*, vol. 28, no. 1, pp. 49–55, 1977, doi: 10.1016/j.carbpol.2011.06.030.

[9] L. Su, J. J. Yin, D. Charles, K. Zhou, J. Moore, and L. (Lucy) Yu, 'Total phenolic contents, chelating capacities, and radical-scavenging properties of black peppercorn, nutmeg, rosehip, cinnamon and oregano leaf', *Food Chem.*, vol. 100, no. 3, pp. 990–997, 2007, doi: 10.1016/j.foodchem.2005.10.058.

[10] I. Tegin, G. Canpolat, and M. Fidan, 'The Antioxidant Capacity, Total Phenolic Content and Phenolic Compounds of Plantago coronopus L. subsp. coronopus in Naturally Distributed in Akdoğmuş-Siirt', Dec. 2018, doi: 10.1109/ISMSIT.2018.8567312.

[11] L. Yu, S. Haley, J. Perret, and M. Harris, 'Antioxidant properties of hard winter wheat extracts', *Food Chem.*, vol. 78, no. 4, pp. 457–461, 2002, doi: 10.1016/S0308-8146(02)00156-5.

[12] L. Müller, K. Fröhlich, and V. Böhm, 'Comparative antioxidant activities of carotenoids measured by ferric reducing antioxidant power (FRAP), ABTS bleaching assay (αTEAC), DPPH assay and peroxyl radical scavenging assay', *Food Chem.*, vol. 129, no. 1, pp. 139–148, Nov. 2011, doi: 10.1016/j.foodchem.2011.04.045.

[13] Uyan Yuksel, Ibrahim Tegin, and Recep Ziyadanogullari, 'Recovery of Copper and Cobalt from Copper Slags as Selective', *J. Environ. Sci. Eng. A*, vol. 6, no. 8, pp. 388–394, Aug. 2017, doi: 10.17265/2162-5298/2017.08.002.

[14] M. Fidan, 'Assessment Of Biological Activity And Element Analysis Of Psylliostachys Spicata (Willd .) Nevski', *J. Anim. Plant Sci.*, vol. 28, no. 6, pp. 1635–1640, 2018.

[15] D. A. Horneck, J. M. Hart, K. Topper, and B. Koepsell, *Methods of soil analysis used in the soil testing laboratory at Oregon State University*. Agr. Exp. Sta. Oregon, USA., 1989.

[16] ISO, 'Soil quality. Determination of phosphorus - Spectometric determination of phosphorus soluble in sodium hydrogen carbonate solution', 1994. https://www.iso.org/obp/ui/#iso:std:iso:11263:ed-1:v1:en (accessed May 28, 2021).

[17] W. . Harrigan, *Laboratory Methods in Food Microbiology*, 3rd ed. California, USA: Academic

Press., 1998.

[18] A. Temiz, *Genel Mikrobiyoloji Uygulama Teknikleri*, 5th ed. Ankara, 2010.

[19] Ş. Tağı, 'Mikrobiyolojik Analiz Yöntemleri', in *Gıda Analizleri*, B. S. . Cemeroğlu, Ed. Ankara: Bizim Grup Basımevi, 2013, pp. 311–383.

[20] A. Halkman, *Gıda Mikrobiyolojisi*. Ankara: Başak Matbaacılık ve Tanıtım Hizmetleri. Ltd, 2019.

[21] F. L. Davies, 'Methods in food and dairy microbiology', *Trends Biotechnol.*, vol. 1, no. 2, pp. 65–66, 1983, doi: 10.1016/0167-7799(83)90074-4.

[22] W. F. Harrigan and M. E. McCance, *Laboratory Methods in Food and Dairy Microbiology*. London: cademic Press Incorporated, 1976.

[23] & L. T. P. Barbosa-Cánovas G V, Fontana Jr A J, Schmidt S J, *Water Activity in Foods*. Oxford, UK: Blackwell Publishing Ltd, 2007.

[24] B. S. Cemeroğlu, *Gıda Analizleri*. Ankara: Bizim Grup Basımevi, 2013.

[25] A. R. Robertson, 'The CIE 1976 Color-Difference Formulae', *Color Res. Appl.*, vol. 2, no. 1, pp. 7–11, 1977, doi: 10.1002/j.1520-6378.1977.tb00104.x.

[26] Hunt, R. W. G. and M. R. Pointer, *Measuring Colour*, 4th ed. UK: John Wiley & Sons, 2011.

[27] K. León, D. Mery, F. Pedreschi, and J. León, 'Color measurement in L*a*b* units from RGB digital images', *Food Res. Int.*, vol. 39, no. 10, pp. 1084–1091, Dec. 2006, doi: 10.1016/j.foodres.2006.03.006.

[28] I. Corp, *IBM SPSS statistics for windows*, Version 22. Armonk, NY: IBM Corp., 2013.

[29] D. E. Pratt and B. J. F. Hudson, 'Natural antioxidants not exploited commercially. In Food Antioxidants', in *Food Antioxidants*, B. J. F. Hudson, Ed. London: Elsevier Applied Science, 1990.

[30] D. Aune *et al.*, 'Fruit and vegetable intake and the risk of cardiovascular disease, total cancer and all-cause mortality-A systematic review and dose-response meta-analysis of prospective studies', *Int. J. Epidemiol.*, vol. 46, no. 3, pp. 1029–1056, Jun. 2017, doi: 10.1093/ije/dyw319.

[31] F. Başoğlu, 'Gıdalarda Kullanılan Bazı Baharatların Mikroorganizmalar Üzerine Etkileri ve Kontaminasyondaki Rolleri', *GIDA*, vol. 7, no. 1, Feb. 1982, Accessed: May 28, 2021. [Online]. Available: https://dergipark.org.tr/tr/pub/gida/91938.

[32] H. J. Damien Dorman, S. G. Deans, R. C. Noble, and P. Surai, 'Evaluation in vitro of plant essential oils as natural antioxidants', *J. Essent. Oil Res.*, vol. 7, no. 6, pp. 645–651, 1995, doi: 10.1080/10412905.1995.9700520.

[33] A. Tomaino *et al.*, 'Influence of heating on antioxidant activity and the chemical composition of some spice essential oils', *Food Chem.*, vol. 89, no. 4, pp. 549–554, Mar. 2005, doi: 10.1016/j.foodchem.2004.03.011.

[34] M. Sabuncu, 'Farklı Turp (raphanus sativus l.) Tiplerinin Antioksidan Kapasite ve Biyoalınabilirliklerinin Belirlenmesi', Bursa Uludağ Üniversitesi, 2019.

[35] M. Fidan, İ. Teğin, M. E. Erez, S. M. Pınar, and H. Eroğlu, 'Total Phenolic-Flovonoid Content, Phenolic Compounds and Elemental Analysis of the Origanum acutidens Plant Used for Ethnobotanical Purpose', *Acad. Platf. J. Eng. Sci.*, vol. 8, no. 1, pp. 41–48, Jan. 2020, doi: 10.21541/apjes.510659.

[36] İ. Teğin, M. Fidan, and M. E. Erez, 'Siirt-Eruh'ta Doğal Yetişen Tecrium polium L. subsp polium'un Antioksidan Kapasitesi, Toplam Fenolik, Flavonoid İçeriği ve Element Analizi', in

AAhtamara I. Uluslararası Multidisipliner Çalışmalar Kongresi, 2018, pp. 486–493.

[37] T. Charoonratana, S. Settharaksa, F. Madaka, and T. Songsak, 'Screening of antioxidant activity and total phenolic content in Raphanus sativus pod', *Int. J. Pharm. Pharm. Sci.*, vol. 6, no. 8, pp. 224–226, 2014, Accessed: May 28, 2021. [Online]. Available: https://innovareacademics.in/journals/index.php/ijpps/article/view/1644/10294.

[38] N. K. Nema, N. Maity, B. K. Sarkar, and P. K. Mukherjee, 'Determination of trace and heavy metals in some commonly used medicinal herbs in Ayurveda', *Toxicol. Ind. Health*, vol. 30, no. 10, pp. 964–968, Dec. 2014, doi: 10.1177/0748233712468015.

[39] G. Yaldız and N. Şekeroğlu, 'Tıbbi ve Aromatik Bitkilerin Bazı Ağır Metallere Tepkisi Gülsüm', *Türk Bilim. Derlemeler Derg.*, vol. 6, no. 1, pp. 80–84, Feb. 2013, Accessed: May 28, 2021. [Online]. Available: www.nobel.gen.tr.

[40] B. Sadık, 'Extraction of some plants in Siirt with subcritic fluid and determination of antioxidant, total phenolic amount and heavy metals of these plant', Siirt University The Graduate School of Natural and Applied Science, Siirt, 2019.

[41] C. Karadaş and D. Kara, 'Chemometric approach to evaluate trace metal concentrations in some spices and herbs', *Food Chem.*, vol. 130, no. 1, pp. 196–202, Jan. 2012, doi: 10.1016/j.foodchem.2011.07.006.

[42] N. S. Rajurkar and M. M. Damame, 'Journal of Radioanalyticat and Nuclear Chemistry', *J. Radioanal. Nucl. Chem.*, vol. 219, no. 1, pp. 77–80, 1997, [Online]. Available: https://idp.springer.com/authorize/casa?redirect_uri=https://link.springer.com/article/10.1007/BF02040269&casa_token=vJUAzo2y58oAAAAA:1rcAavEKojUjEepwHC-8b0TJ3tLjwfQHlKPb4E90xeWvzLKBKM0HArXowoclMI_T-G3f4Rq9m-eopHzUQQ.

[43] N. G. Babu, S. S. Ram, M. Sudershan, N. L. Das, N. Nagar, and W. Bengal, 'Estimation of elemental concentrations of Indian medicinal plants using energy dispersive X-ray fluorescence (EDXRF) technique', vol. 3, no. 3, pp. 299–304, 2016.

[44] A. Temiz, 'Gıdalarda mikrobiyal gelişmeyi etkileyen faktörler', in *Gıda Mikrobiyolojisi*, 4th ed., Ünlütürk A & Turantaş F, Ed. Çınarlı-İzmir: Mengi Tan Basımevi, 2015, pp. 52–83.

[45] M. Adams and R. Mitchell, 'Fermentation and pathogen control: A risk assessment approach', in *International Journal of Food Microbiology*, Nov. 2002, vol. 79, no. 1–2, pp. 75–83, doi: 10.1016/S0168-1605(02)00181-2.

[46] B. Uymaz Tezel and P. Şanlıbaba, 'Fermente Gıdalar: Mikrobiyoloji, Teknoloji ve Sağlık', in *Probiyotik Mikroorganizmalar*, 1st ed., Anlı E & Şanlıbaba P, Ed. Ankara: Nobel Akademik Yayıncılık Eğitim Danışmanlık Tic. Ltd. Şti, 2019, pp. 619–647.

[47] M. Cano-Lamadrid, L. Trigueros, A. Wojdyło, A. Carbonell-Barrachina, and E. Sendra, 'Anthocyanins decay in pomegranate enriched fermented milks as a function of bacterial strain and processing conditions', *LWT - Food Sci. Technol.*, vol. 80, pp. 193–199, Jul. 2017, doi: 10.1016/j.lwt.2017.02.023.

[48] A. J. Marsh, C. Hill, R. P. Ross, and P. D. Cotter, 'Fermented beverages with health-promoting potential: Past and future perspectives', *Trends in Food Science and Technology*, vol. 38, no. 2. Elsevier Ltd, pp. 113–124, Aug. 01, 2014, doi: 10.1016/j.tifs.2014.05.002.

[49] Anonim, 'TS 11149 Şalgam Suyu Standardı', Ankara, 2003. Accessed: May 30, 2021. [Online]. Available: https://intweb.tse.org.tr/standard/standard/Standard.aspx?053107106111065067115113049116090107100056052055108081090071086075069085047110067109075073081116103090081086073108065117084119101076057109074053067116072069049121081079087100070

104122114120071.

[50] M. Karapınar and Ş. Aktuğ Gönül, 'Gıda kaynaklı mikrobiyal hastalıklar', in *Gıda Mikrobiyolojisi*, 3rd ed., A. Ünlütürk and F. . Turantaş, Eds. İzmir: Türkiye: Mengi Tan Basımevi., 2015, pp. 109–164.

[51] C. Bontsidis *et al.*, 'Microbiological and chemical properties of chokeberry juice fermented by novel lactic acid bacteria with potential probiotic properties during fermentation at 4◦c for 4 weeks', *Foods*, vol. 10, no. 4, p. 768, Apr. 2021, doi: 10.3390/foods10040768.

[52] H. Ç. Kaymak, 'Turp (Raphanus sativus L.)'ta Bazı Gelişme Özellikleri ve Verimin Vernalizasyon Süresi, Gün Uzunluğu, Ekim ve Hasat Zamanı ile İlişkisi', Atatürk Üniversitesi Fen Bilimleri Enstitüsü, Erzurum, 2006.

Open Journal of Nano
ISSN: 2147-0081
(2022) 7–1
Research Article / Araştırma Makalesi

Optimization of Cutting Parameters Affecting Cutting Force and Surface Roughness in Machining of AISI P20 Die Steel

[1] Mahir Akgün, [2] Barış Özlü

[1]Department of Machine and Metal Technology, Technical Sciences Vocational School, Aksaray University, Aksaray, Turkey
Corresponding author, e-mail: mahirakgun@aksaray.edu.tr

Submission Date: 21.12.2021 Acceptation Date: 09.02.2022

Abstract - This study focuses on optimizing cutting parameters effective on cutting force (Fc) and surface roughness (Ra) in the machining of AISI P20 steel. The turning experiments have been performed in CNC lathe at three different cutting speeds (Vc) (120, 180, and 240 m/min), three different feed rates (f) (0.12 0.21 and 0.3 mm/rev), and three different depths of cut (a) (0.4, 0.8, and 1.2 mm) according to Taguchi L9 orthogonal array. The effect levels of the cutting parameters on Fc and Ra have been determined with analysis of variance (Anova). The analysis results indicate that the depth of cut is the most significant parameter affecting Fc while the feed rate is the most significant parameter affecting Ra. Moreover, the result analysis shows that cutting speed of 240 m/min, feed rate of 0.12 mm/rev, and depth of cut of 0.4 mm) factor levels were the optimum cutting parameters for the output parameters (Fc and Ra). In turning experiments performed at optimum cutting parameters, the lowest Fc and Ra values were measured as 178N and 0.412 µm, respectively.

Keywords: AISI P20 steel, Cutting Force, Surface Roughness, Optimization

AISI P20 Kalıp Çeliğinin İşlenmesinde Kesme kuvveti ve Yüzey Pürüzlülüğünü Etkileyen Kesme Parametrelerinin Optimizasyonu

Öz- Bu çalışma, AISI P20 çeliğinin işlenmesinde kesme kuvveti (Fc) ve yüzey pürüzlülüğü (Ra) üzerinde etkili olan kesme parametrelerinin optimize edilmesine odaklanmaktadır. Tornalama deneyleri Taguchi L9 ortogonal dizisine göre üç farklı kesme hızında (Vc) (120, 180 ve 240 m/dak), üç farklı ilerleme hızında (f) (0.12 0.21 ve 0.3 mm/dev) ve üç farklı talaş derinliğinde a) (0,4, 0,8 ve 1,2 mm) CNC torna tezgahında gerçekleştirilmiştir. Kesme parametrelerinin Fc ve Ra üzerindeki etki düzeyleri varyans analizi (Anova) ile belirlenmiştir. Analiz sonuçları, talaş derinliğinin kesme kuvvetini etkileyen en önemli parametre olduğunu, ilerleme hızının ise yüzey pürüzlülüğünü etkileyen en önemli parametre olduğunu göstermektedir. Dahası, analiz sonuçlar, 240 m/dk kesme hızı, 0.12 mm/dev ilerleme hızı ve 0.4 mm talaş derinliği çıktı parametreleri (Fc ve Ra) için optimum kesme parametreleri olduğunu göstermektedir. Optimum kesme parametrelerinde yapılan tornalama deneylerinde en düşük Fc ve Ra değerleri sırasıyla 178N ve 0.412 µm olarak ölçülmüştür.

Anahtar kelimeler: AISI P20 çelik, Kesme kuvveti, Yüzey Pürüzlülüğü, Optimizasyon

[1] Corresponding author: Tel: 0 382 288 20 16
E-mail: mahirakgunaksaray.edu.tr

Open Journal of Nano
ISSN: 2147-0081
(2022) 7–1
Research Article / Araştırma Makalesi

1. Introduction

In today's conditions, many mass-produced parts are created using molds and mold elements. In particular, considering the use of thermoplastics, the importance of the molding sector is understood. Moreover, the quality, cost and lead times of molds are critical to the economics of many industries. For example, in the automotive industry, it affects produce a large number of components, subassemblies, and assemblies. Therefore, it focuses on process modeling, rapid prototyping, rapid tooling, high-speed cutting and optimized toolpath creation for hard machining with the developing technology in this field [1, 2].

AISI P20 steel, which is plastic mold steel, is used in applications such as plastic extrusion, plastic injection, and blow molding. The very important properties of these steels are hardness, strength, high toughness, very good polishability, weldability, and suitability for nitration. However, the formation of built-up edge (BUE) in the machining process of this steel seriously affects the cutting tool life and production efficiency [3]. Moreover, it is difficult to machine these steels, which are alloyed with strong carbide forming elements such as Mo and Cr [4]. on the other hand, in the mold manufacturing industry, it is desired to produce the molds with the best surface quality in a short time. Therefore, in order to obtain high cutting performance in mold production, optimum levels of cutting parameters should be selected. However, cutting conditions are generally determined by an operator's experience or practical knowledge [5]. Tooling cost and time loss are increased in this way. For these reasons, it is very important to define the most suitable cutting conditions in terms of surface quality and cutting forces, which are essential machinability criteria for production efficiency [6-9]. For example, Davim was investigated the effect of cutting parameters and cutting time on drilling metal-matrix composites using the Taguchi method [10]. Statistical results indicate that the cutting time was the factor which had the greatest influence on the tool wear (50%), followed by the feed rate (24%). Mandal et al. were investigated the machinability of AISI 4340 steel with newly-developed zirconia-toughened alumina ceramic inserts [11]. The Taguchi method, the signal-to-noise ratio, and analysis of variance have been applied to study the performance characteristics. Statistical results indicate that the depth of cut is a maximum contribution to tool wear. Akkuş and Yaka applied the Taguchi method to investigate the effect of cutting parameters on turning AISI 1040 steel [12]. The analysis of the results showed that feed rate had the most significant effect on surface roughness. Ballıkaya and Altuğ were used the Taguchi method to determine the optimal process parameters in machining hardened D2 cold work tool steel using wire erosion (WEDM) method [13]. The orthogonal array, the signal-to-noise ratio, and analysis of variance were employed to study the performance characteristics (the machined surface hardness and the regenerated white layer thickness). Statistical results indicate that the most effective parameter on the white layer thickness is the commercial and heat-treated sample parameter (57.236%). In the cut surface hardness values, the most effective parameter was the sample parameter (98.627%). Akkuş and Yaka, investigated the effect of cutting parameters on surface roughness, vibration, and energy consumption in the machining of titanium 6Al-4V ELI (grade 5) alloy [14]. The analysis of the results showed that the effective parameter in surface roughness, vibration and energy consumption is feed rate.

From the literature review, it is seen that optimization techniques are used to estimate output parameters and optimization of input parameters in machining operations (turning, milling, drilling, etc.). Furthermore, it has been determined that the studies on the machinability of AISI P20 plastic mold steel are limited. In the present study, the machinability of AISI P20 mold steel, which is widely used in the mold industry, was evaluated in terms of main cutting force (Fc) and surface roughness (Ra). Machinability tests were carried out on a CNC lathe according to the Taguchi L9 index. S/N analysis and analysis of variance were used to determine ideal cutting conditions and the effects of cutting parameters on output parameters (Fc and Ra), respectively.

Open Journal of Nano
ISSN: 2147-0081
(2022) 7–1
Research Article / Araştırma Makalesi

2. Materials and Methods

In the study, AISI P20 steel with a diameter of 30 mm and a length of 300 mm was used as the workpiece material. Table 1 shows the chemical composition of the workpiece material used in the experiments. Turning experiments were performed on Johnford TC-35 CNC lathe under dry cutting conditions. Kistler 9257A type dynamometer and equipment's were used to measure the main cutting force (Fc). Force measurement system; it consists of 9257A dynamometer, Kistler 5070A amplifier, data acquisition card, and "DynoWare Type 2825Ai-2" software for collecting cutting force signals. The experimental setup is schematically shown in Fig. 1. In the analysis of cutting forces, the main cutting force (Fc) values, which are of primary importance in terms of energy consumption in machining operations, were taken into account.

Table 1. Chemical composition (%) of the workpiece material

Elements	C	Si	Mn	Cr	Ni	Mo
Wt.%	0.1	0.3	2.5	3.00	1.0	0.3

In the turning experiments, carbide cutting tools, which were coated with TiCN/Al2O3 using the CVD method and produced by Kennametal in KCM15 quality and CNMG120408UP geometry, were used. The turning parameters and levels used in the experiments are given in Table 2. Roughness measurements were made on the machined surfaces using the MAHR-Perthometer-M1 portable surface roughness (Ra) device. After each measure, the workpiece was rotated 90º on its axis, and the average Ra value was determined by taking the arithmetic average of the four measurements.

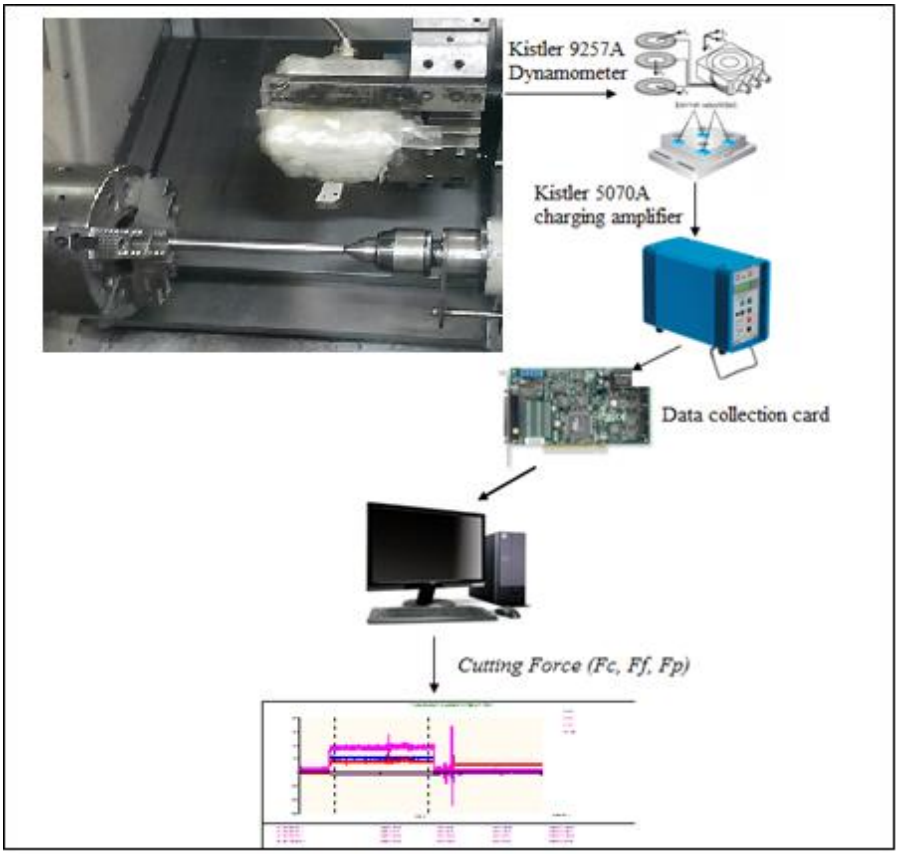

Figure 1. Experimental setup used for the measurement of cutting force

Open Journal of Nano
ISSN: 2147-0081
(2022) 7–1
Research Article / Araştırma Makalesi

Table 2. Cutting parameters and levels.

Code	Cutting Parameters	Units	Level 1	Level 2	Level 3
A	Cutting speed (Vc)	(m/min)	120	180	240
B	Feed rate (f)	(mm/rev)	0.12	0.21	0.3
C	Depth of cut (ap)	(mm)	0.4	0.8	1.2

3. Experimental Design and Optimization

In the manufacturing industry, different optimization methods are used in material processing to minimize product costs and increase efficiency [15]. Taguchi method, which is one of the optimization methods, is used to reduce the product development time and the relative costs [16]. In this study, Taguchi method was used in designing the experiments and determining the optimum cutting parameters. In this context, turning experiments were designed according to Taguchi's L9 (3^3) orthogonal array and the signal-to-noise (S/N) ratio was calculated to determine the optimum cutting parameters [17]. The "smallest best" approach in Eq. (1) was used to calculate the signal-to-noise (S/N) ratios because it was aimed to determine the optimum cutting parameters to obtain the lowest levels of Fc and Ra in the study.

$$n = \frac{\mathrm{S}}{\mathrm{N}} = -10\log\left(\frac{1}{n}\sum_{i=1}^{n} y_i^2\right) \quad (1)$$

Moreover, analysis of variance (ANOVA) was applied to determine the effects of cutting parameters on the main cutting force (Fc) and surface roughness (Ra) values.

4. Results and Discussions

4.1 Analysis of the signal-to-noise (S/N) ratio

Cutting force (Fc) and surface roughness (Ra) have been measured in experiments designed by using the Taguchi technique, optimization of the measured output parameters has been provided by signal-to-noise (S/N) ratios. The lowest values of Ra and Fc are significant for improving the product's quality and the dynamics of the machine tool, respectively. For this reason, the “lower-the-better” equation was used for the calculation of the S/N ratio. Table 3 shows the Fc and Ra values obtained after processing and their corresponding S/N ratios. At the end of the turning tests, the average values of the Fc and Ra have been calculated to be 230.07N and 0.668 µm respectively. Similarly, average values of S/N ratio for surface roughness and flank wear were calculated to be -48.2 dB and 3.583 dB respectively.

Table 3. Experiment results and S/N ratios values

Id No	Experiment Code	Fc (N)	SN-Fc (N)	Ra (µm)	SN-Ra (µm)
1	$A_1B_1C_1$	218.50	-46.789	0.550	5.1927
2	$A_1B_2C_2$	275.00	-48.786	0.670	3.4785
3	$A_1B_3C_3$	332.62	-50.438	0.765	2.3267
4	$A_2B_1C_2$	240.55	-47.604	0.620	4.1521
5	$A_2B_2C_3$	272.54	-48.691	0.720	2.8533
6	$A_2B_3C_1$	315.47	-49.977	0.765	2.3267
7	$A_3B_1C_3$	185.98	-45.343	0.650	3.7417
8	$A_3B_2C_1$	230.05	-47.234	0.500	6.0206
9	$A_3B_3C_2$	284.35	-48.943	0.780	2.1581

Analysis of the effect of each input factor (Vc, f, ap) on the output parameters was performed with a “S/N response table”. The response tables of S/N for Ra and Fc are given in Table 4. According to

Open Journal of Nano
ISSN: 2147-0081
(2022) 7–1
Research Article / Araştırma Makalesi

Table 4, A cutting speed 240 m/min (level 3), B feed rate 0.12 mm/rev (level 1) and C depth of cut 0.4 mm (level 1) were defined as ideal cutting parameters for both Fc and Ra. In turning experiments performed at optimum cutting parameters, the lowest Fc and Ra values were measured as 178N and 0.412 µm, respectively. In a similar study, Gupta et al. reported that cutting speed of 160 m/min, nose radius of 0.8 mm, feed of 0.1 mm/rev, depth of cut of 0.2 mm and the cryogenic environment were the most favorable cutting parameters for high-speed CNC turning of AISI P-20 tool steel [18].

Table 4. Answer table for Fc and Ra

Code	Factors	Level 1	Level 2	Level 3	Delta	Rank
Fc						
A	Vc	-48.67	-48.76	**-47.17**	1.58	2
B	f	**-46.58**	-48.24	-49.79	3.21	1
C	ap	**-48.00**	-48.44	-48.16	0.44	3
Ra						
A	Vc	3.666	3.111	**3.973**	0.863	3
B	f	**4.362**	4.117	2.271	2.092	1
C	ap	**4.513**	3.263	2.974	1.539	2

The graphic form of the level values of the control factors for Fc and Ra is shown in Figure 2. When Figure 2 is examined, it is seen that the output parameters (Fc and Ra) increase with increasing feed rate and depth of cut and decrease with increasing cutting speed.

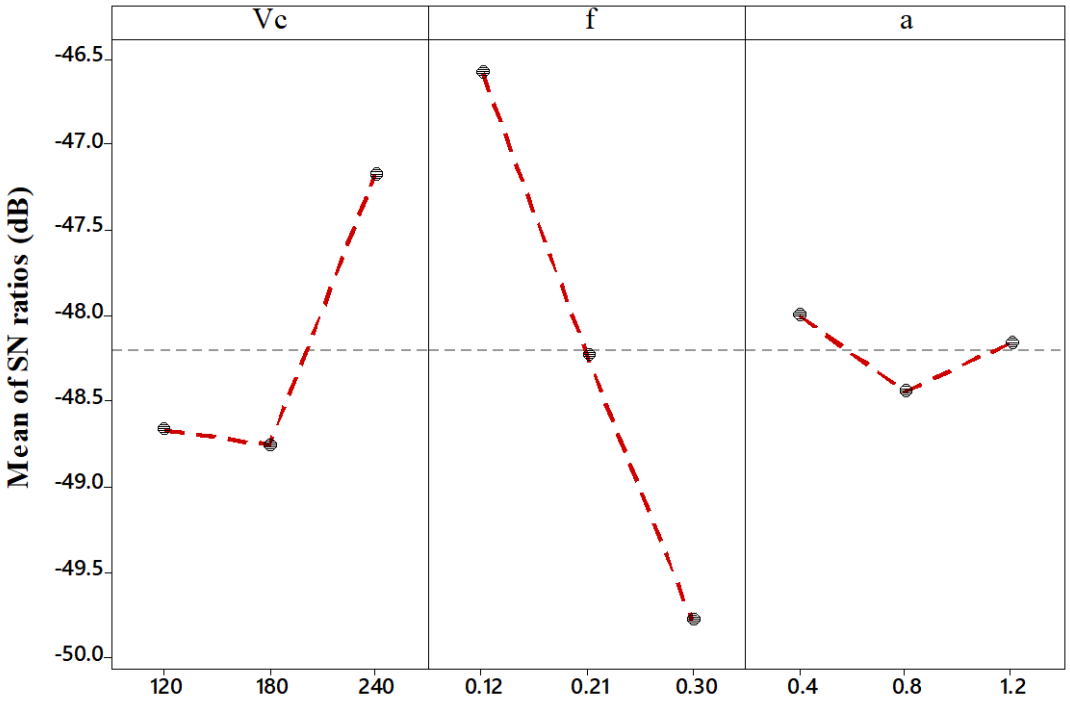

(a)

Open Journal of Nano
ISSN: 2147-0081
(2022) 7–1
Research Article / Araştırma Makalesi

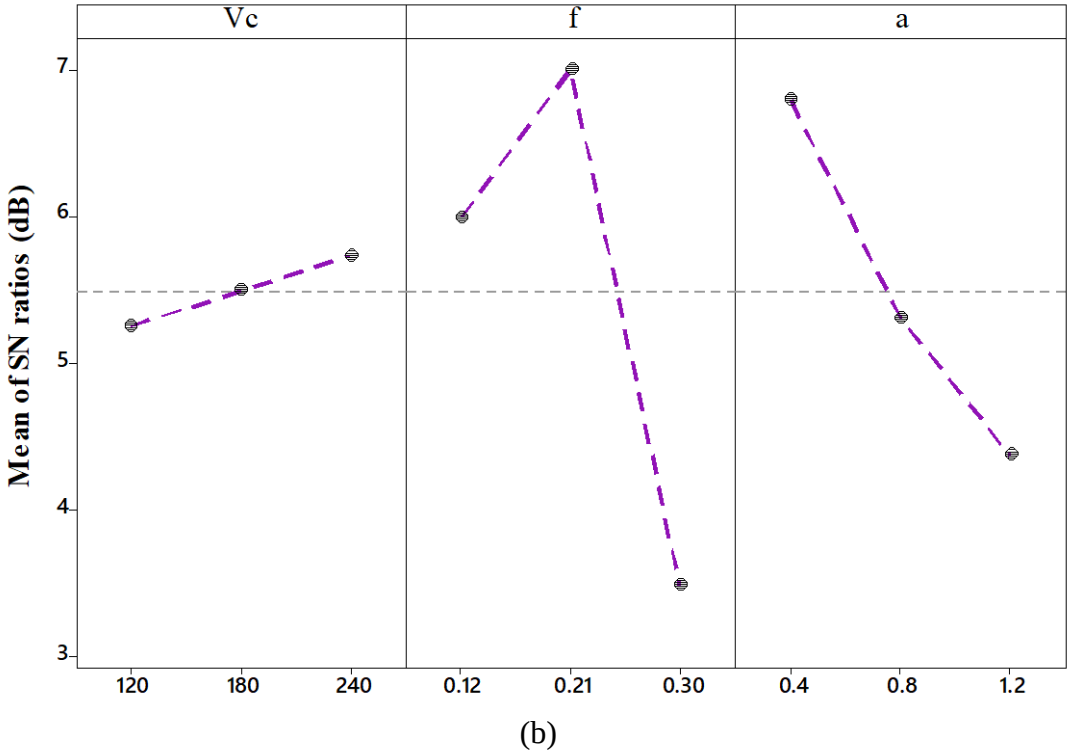

(b)

Figure 2. Effect of process parameters on average S/N ratio for a) Fc and b) Ra.

4.2 Evaluation of experimental results

The changes in the Fc and Ra obtained as the result of the experimental study are seen in Figs. 3 and 4, respectively. The measured Fc values ranged from 150 to 320N, and the measured Ra values ranged from 0.4098 to 1.626 µm. When Figs. 3 and 4 is examined, it is seen that the Fc and Ra increases depending on the increase in the feed rate in the machining of AISI P20 steel. The Fc values are about 35% increase with increasing feed rate from 0.1 mm/rev to 0.15 mm/rev while 45% increase by feed rate from 0.15 mm/rev to 0.2 mm/rev. Similarly, The Ra values are about 40% increase with increasing feed rate from 0.1 mm/rev to 0.15 mm/rev while 50% increase by f from 0.15 mm/rev to 0.2 mm/rev. The experimental findings showed that the highest Fc and Ra values were measured at the highest level of the feed rate (0.2 mm/rev). Another indicator of the significant effect of the feed rate on the output parameters is the 76.10% and 59.39% contribution rates for Fc and Ra in the ANOVA analysis, respectively. It is thought that this situation is caused by the increase in the loads on the cutting tool as a result of the increase in the chip cross-section due to the increase in the feed rate [19-21]. When the tool wear images in Fig. 5 are examined, it is seen that the nose and flank wear increases with the increase in the feed rate. Consequently, this deformation in the cutting tool affects the output parameters negatively. Similarly, Yaşar et al. in the experimental and numerical analysis of cutting force in the turning of AISI P20 reported that Fc increased with the increase in feed rate [22]. On the other hand, it can be said that the Fc and Ra values slightly decrease with the increase in cutting speed. However, there is no significant change with increasing cutting speed at high feed rates (0.21 mm/rev and 0.30 mm/rev). Aggarwal et al. in turning AISI P20 tool steel using liquid nitrogen as a coolant reported that for low cutting force and surface roughness, a high cutting speed range (160-200 m/min) and a low to medium feed rate range (0.10-0.12 mm/rev) should be selected [23].

Open Journal of Nano
ISSN: 2147-0081
(2022) 7–1
Research Article / Araştırma Makalesi

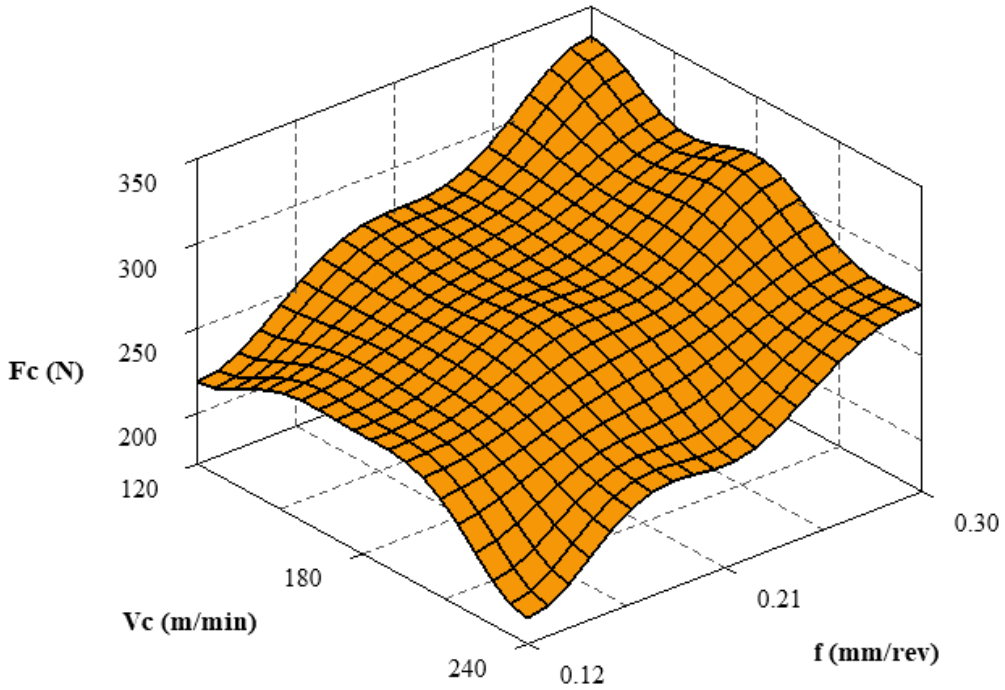

Figure 3. Effect of cutting parameters on Fc

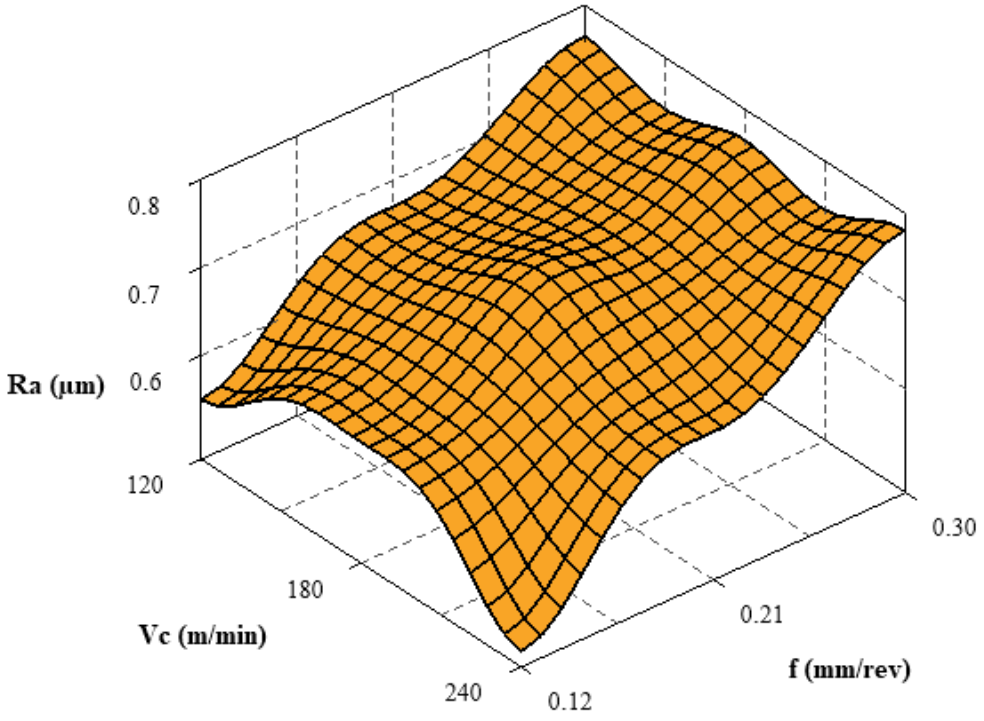

Figure 4. Effect of cutting parameters on Ra

Open Journal of Nano
ISSN: 2147-0081
(2022) 7–1
Research Article / Araştırma Makalesi

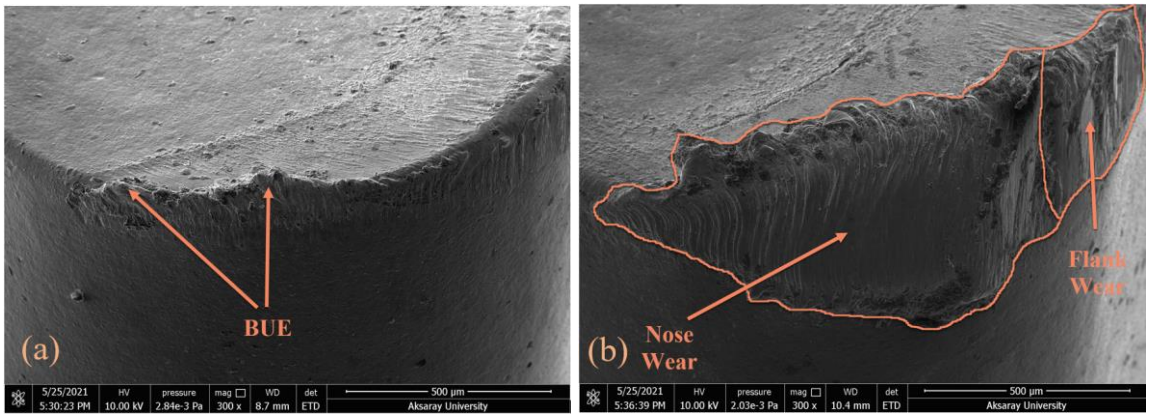

Figure 5. SEM images of cutting tools (a) 240 m/min, 0.12 mm/rev and 0.8 mm depth of cut (b) 240 m/min, 0.30 mm/rev and 0.8 mm depth of cut

4.3 Analysis of variance (ANOVA) results

ANOVA was used to analyze the effects of cutting speeds, feed rates, and depths of cut on output parameters (Fc and Ra). The ANOVA results for the output parameters (Fc and Ra) are shown in Table 5. This analysis was carried out a 5% significance level and a 95% confidence level. In the table, F values and percentage contribution rate were used to determine the importance of each factor on the output parameters. Considering the F values, the factor with the largest F value is most influences the output parameter. According to Table 5, the percent contributions of the Vc, f and ap factors on the Fc were found to be 21.74%, 76.10%, and 1.04%, respectively. Consequently, the most important parameter affecting the Fc was feed rate (factor B, 76.10%). On the other hand, the percent contributions of the Vc, f and ap factors on the Ra were found to be 6.77%, 59.39%, and 24.19%, respectively. This showed that the most effective factor on Ra was feed rate (factor B, 59.39%). The percent of error was considerably low at 1.24% and 9.65% for Fc and Ra, respectively.

Table 5. Variance results for Fc and Ra

Factors	DF	Seq SS	Adj MS	F-Value	P-Value	Contribution (%)
Fc						
Vc	2	3857.6	1928.81	19.35	0.049	21.74
f	2	13507.6	6753.53	67.75	0.015	76.10
ap	2	184.1	92.05	0.92	0.520	1.04
Error	2	199.4	99.68	-	-	1.12
Total	8	17748.1	-	-	-	100.00
Ra						
Vc	2	0.00533	0.00266	0.7	0.588	6.77
f	2	0.04682	0.02341	6.16	0.140	59.39
ap	2	0.19072	0.00953	2.51	0.285	24.19
Error	2	0.00760	0.00380	-	-	9.65
Total	8	0.07883	-	-	-	100

5. Conclusions

In this study, an experimental investigation was performed to analyze the effects of the cutting parameters on surface roughness (Ra) and cutting force (Fc) in the machining AISI P20 steel. Moreover, the optimum cutting conditions were determined by the Taguchi method. The following conclusions may be drawn from this study:

- Generally, with increasing feed rate, the surface roughness and the main cutting force (Fc) values were increased.

- According to the S/N ratios, it was concluded that the A3B1C1 (cutting speed 240 m/min, feed rate 0.12 mm/rev, and depth of cut 0.4 mm) factor levels were the optimum cutting parameters for the main cutting force and surface roughness. In turning experiments performed at optimum cutting parameters, the lowest Fc and Ra values were obtained as 178N and 0.412 µm, respectively.
- The variance results indicate that the depth of cut was the parameter affecting the main cutting force while the feed rate was the most significant factor affecting surface roughness with a percentage contribution of 74.6% and 59.39%, respectively.
- Medium cutting velocity and feed rate could be recommended for use in the turning of AISI P20 plastic mold steel.

Peer-review: Externally peer - reviewed.

Author contributions: Concept – M.A, B. Ö.; Data Collection &/or Processing – M.A, B. Ö.; Literature Search – B.Ö. Writing – M. A.

Conflict of Interest: This paper has been presented at the ICENTE'21 (5th International Conference on Engineering Technologies) held in Konya (Turkey), November 18-20, 2021.)

Financial Disclosure: The authors declared that this study has received no financial support.

References

[1] Altan, T., Lilly, B., Yen, Y. C., 2001. Manufacturing of Dies and Molds. CIRP Ann. 50, 404–422.

[2] Senevirathne, S. W. M. A. I., Punchihewa, H. K. G., 2018. Reducing surface roughness by varying aerosol temperature with minimum quantity lubrication in machining AISI P20 and D2 steels. Int. J. Adv. Manuf. Technol. 94, 1009–1019.

[3] Ravi, S., Gurusamy, P., 2021. Cryogenic machining of AISI p20 steel under liquid nitrogen cooling. Mater. Today Proc. 37, 806–809.

[4] Demir, H., Gündüz, S., Erden, M. A., 2018. Influence of the heat treatment on the microstructure and machinability of AISI H13 hot work tool steel. Int. J. Adv. Manuf. Technol. 95, 2951–2958.

[5] Aslan, D., & Budak, E., 2014. Semi-analytical Force Model for Grinding Operations. Procedia CIRP 14, 7–12.

[6] Zeilmann, R. P., Nicola, G. L., Vacaro, T., Teixeira, C. R., Heiler, R., 2012. Implications of the reduction of cutting fluid in drilling AISI P20 steel with carbide tools. Int. J. Adv. Manuf. Technol. 58, 431–441.

[7] Outeiro, J. C., 2012. Optimization of Machining Parameters for Improved Surface Integrity of AISI H13 Tool Steel. in Machines et Usinage a Grande Vitesse (MUGV).

[8] Kıvak, T., 2014. Optimization of surface roughness and flank wear using the Taguchi method in milling of Hadfield steel with PVD and CVD coated inserts. Measurement 50, 19–28.

[9] Kara, F., Öztürk, B., 2019. Comparison and optimization of PVD and CVD method on surface roughness and flank wear in hard-machining of DIN 1.2738 mold steel. Sens. Rev. 39, 24–33.

[10] Davim, J. P., 2003. Study of drilling metal–matrixcomposites based on the Taguchi techniques, J. Mater. Processing Technol 132, 3250–3254.

[11] Mandal, N., Doloi, B., Mondal, B., Das, R., 2011. Optimization of flank wear using Zirconia Toughened Alumina (ZTA) cutting tool: Taguchi method and regression analysis, Measurement 44, 2149–2155.

[12] Akkuş, H., Harun, Y., 2018. Optimization of turning process by using taguchi method. Sakarya University Journal of Science 22(5), 1444-1448.

[13] Ballıkaya, H., Altuğ, M., 2021. Isıl işlem görmüş D2 Soğuk İş Takım Çeliğinin Tel Erozyonda İşlenmesinde Kesme Parametrelerinin Beyaz Tabaka kalınlığı ve Yüzey Sertliğine Etkisi. International Journal of Innovative Engineering Applications 5 (2), 181-186.

[14] Akkuş, H., Yaka, H., 2021. Experimental and statistical investigation of the effect of cutting parameters on surface roughness, vibration and energy consumption in machining of titanium 6Al-4V ELI (grade 5) alloy. Measurement 167, 108465.

[15] Nas, E., Özbek, N. A., 2019. Optimization of the Machining Parameters in Turning of Hardened Hot Work Tool Steel Using Cryogenically Treated Tools. Surf. Rev. Lett. 1950177, (2019).

[16] Palanikumar, K., 2011. Experimental investigation and optimisation in drilling of GFRP composites. Measurement 44, 2138–2148.

[17] Asiltürk, İ., Akkuş, H., 2011. Determining the effect of cutting parameters on surface roughness in hard turning using the Taguchi method. Measurement 44(9), 1697-1704.

[18] Gupta, A., Singh, H., Aggarwal, A., 2011. Taguchi-fuzzy multi output optimization (MOO) in high-speed CNC turning of AISI P-20 tool steel. Expert Syst. Appl. 38, 6822–6828.

[19] Özlü, B., Demir, H., Türkmen, M., 2019. The effect of mechanical properties and the cutting parameters on machinability of AISI 5140 steel cooled at high cooling rates after hot forging. Politek. Derg. 22, 879–887.

[20] Akgün, M., Kara, F., 2021. Analysis and Optimization of Cutting Tool Coating Effects on Surface Roughness and Cutting Forces on Turning of AA 6061 Alloy. Advances in Materials Science and Engineering, 2021, 6498261.

[21] Akgün, M., Demir, H., 2021. Optimization of Cutting Parameters Affecting Surface Roughness in Turning of Inconel 625 Superalloy by Cryogenically Treated Tungsten Carbide Inserts. SN Applied Sciences, 3(2), 1-12.

[22] Yaşar, N., Sekmen, M., Korkmaz, M. E., 2016. "AISI P20 Çeliğinin İşlenmesinde Kesme Kuvvetinin Deneysel ve Nümerik Analizi," Gazi Üniversitesi Fen Bilim. Derg. Part C, Tasarım Ve Teknol. 4(1), 13–19.

[23] Aggarwal, A., Singh, H., Kumar, P., Singh, M., 2008. Optimization of multiple quality characteristics for CNC turning under cryogenic cutting environment using desirability function. Journal of materials processing technology 205(1-3), 42-50.